RSC Advances

PAPER

View Article Online
View Journal | View Issue

Cite this: *RSC Adv.*, 2021, **11**, 12117

Prediction of emulsification behaviour of pea and faba bean protein concentrates and isolates from structure–functionality analysis†

Fatemeh Keivaninahr,[a] Pravin Gadkari,[a] Khaled Zoroufchi Benis,[b] Mehmet Tulbek[c] and Supratim Ghosh *[a]

The effects of different extraction methods on the structure–functionality and emulsification behaviour of pea and faba bean protein isolates, and concentrates were studied at pH 7 and 2, and a regression model was developed to predict emulsion characteristics based on protein properties. The concentrates produced by air classification had lower protein content but higher solubility in water compared to the isolates produced by isoelectric precipitation. The protein secondary structure did not show a consistent difference; however, much higher intrinsic fluorescence was observed for the soluble compared to the insoluble fractions. Interfacial tension of all faba proteins was lower than pea, while there was no significant difference between the concentrates and isolates. The higher protein content of the isolates was found to improve their water holding capacity. Canola oil (40 wt%)-in-water coarse emulsions, prepared with 2 wt% proteins and 0.25 wt% xanthan gum showed smaller particle size at pH 7 than pH 2, while the zeta potential, viscosity and gel strength were higher at pH 7. Emulsions stabilized with concentrates were better or comparable to the isolates in terms of particle size, zeta potential, and microstructure. The regression model predicted that an increase in solubility, intrinsic fluorescence, water and oil holding capacities are more favourable to decrease emulsion particle size, while an increase in solubility, intrinsic fluorescence would lead to higher emulsion destabilization. A decrease in interfacial tension was more favourable to lower destabilization. Emulsion viscosity was more dependent on water holding capacity compared to any other factor. Such models could be extremely beneficial for the food industry to modulate processing for the development of desired pulse protein ingredients.

Received 1st November 2020
Accepted 7th February 2021

DOI: 10.1039/d0ra09302e

rsc.li/rsc-advances

1. Introduction

Plant proteins are gaining more interest, across the globe, due to their wide range of applications in plant-based food systems.[1,2] In the food industry, plant proteins are used to replace animal proteins to meet consumer demand, improve nutritional quality, and maintain similar functionality and sensory characteristics (*i.e.* texture, flavour, and colour).[3] Protein concentrates and isolates from soybean and wheat are widely used in the food industry. However, dry legumes or pulses, as a critical and inexpensive product, are fast emerging as a popular source of plant proteins in food.[4] Pulses are rich in proteins, starch, fibre, vitamins and minerals. In recent years, they are being considered as alternative protein sources to replace animal and soybean proteins due to their higher protein content, lower cost, lower allergenicity and wider acceptability.[5]

Numerous methods for the extraction of proteins from pulse flours are being studied to optimize the quantity while maximizing the quality.[6–8] In general, protein extraction processes can be classified into dry and wet methods.[1] In the dry processing, the flour is finely milled, and then the large starch granules are separated from the smaller protein-rich particles by air classification based on size, shape and density.[9] For complete separation of protein that still adheres to the starch granules, a second milling step is also used, which may increase the presence of damaged starch. The major advantages of dry processing are maintaining the functionality of native protein, lower energy and water use. However, the products of dry processing, the protein concentrates, are usually lower in protein content (up to 50–60% protein).[10] In wet processing, two of the most commonly used methods are acid/alkali extraction–isoelectric precipitation and salt extraction (SE).[8] The process of acid/alkali extraction–isoelectric precipitation starts by solubilizing pulse flour under alkaline or acidic conditions followed by centrifugation to separate the soluble protein fraction.[11]

[a]*Department of Food and Bioproduct Sciences, College of Agriculture and Bioresources, University of Saskatchewan, 51 Campus Drive, Saskatoon, S7N 5A8, SK, Canada. E-mail: supratim.ghosh@usask.ca*

[b]*Department of Chemical and Biological Engineering, University of Saskatchewan, Saskatoon, SK, Canada*

[c]*AGT Foods, Saskatoon, Saskatchewan, Canada*

† Electronic supplementary information (ESI) available. See DOI: 10.1039/d0ra09302e

Then, the protein is precipitated by adjusting the pH to its isoelectric point (pI) and separated from the rest of the solution.[12] Finally, the precipitated protein is re-solubilized by adjusting to pH 7 and dried.[13] The final protein isolates are rich in purity (usually 80–90% protein), but the major drawback is the loss of the native functionality of the proteins.[10] In the SE, proteins are extracted by the salting-out process, which leads to protein separation followed by de-salting using micellization or dialysis and recovery of the protein isolate *via* precipitation and drying.[1,14] The behaviour of proteins in food is affected by their structure, conformation, physicochemical properties and interaction with other food components and the nature of the environment.[15,16] These properties, in turn, depends on the processing methods used during protein extraction; hence, the behaviour of a pulse protein in food would largely depend on the choice of ingredients, concentrates or isolates. For example, a lower protein content, higher protein solubility, foaming capacity and gelling ability of the dry-fractionated faba bean protein (FBP) compared to the isolate produced by acid/alkali extraction–isoelectric precipitation was observed.[17] Karaca *et al.*[6] found that the isoelectric-precipitated chickpea and lentil protein isolates had higher surface charges and formed emulsions with smaller droplet size than the SE isolates. Emulsification is one of the most critical functionalities of food proteins. During emulsification, proteins stabilize dispersed oil droplets by lowering the interfacial tension (IT), covering the droplets with a protein layer and preventing coalescence by forming a strong viscoelastic membrane.[18] The carbohydrates present in the protein concentrate, or isolates, remain dispersed in the continuous phase and act as a viscosity enhancer and bulky barriers between the oil droplets, preventing emulsion destabilization.[19] Moreover, the excess unabsorbed biopolymers may also act as depletant and induce depletion flocculation in beverage emulsions.[20]

These functionalities of proteins might also be affected by the exposure to severe environmental conditions during food processing (such as thermal treatment, the addition of salt, extreme pH conditions, organic solvents and surfactants) that can change their structure, leading to protein denaturation.[21] The thermal treatment has been used to improve functionality by resolving the "beany flavour" problem of faba bean by inactivating the peroxidase and lipoxygenase.[22] However, a progressive decrease in oil emulsification was observed by heating pea protein concentrate (PPC).[23] Pressure or thermally induced unfolding of the 11S globulin *Vicia faba* protein led to the formation of emulsions with larger droplets than those made with the native protein.[24] Protein aggregation of pea proteins (PP) was shown to increase by thermal treatment; however, emulsions were formed with higher protein adsorption and creaming stability than those formed with unheated proteins.[25]

In spite of such a wide range of research on plant proteins, there is a lack of studies that directly compared concentrates and isolates. Therefore, it is difficult for the food industry to clearly understand the advantages or disadvantages of the available protein ingredients. To address this challenge, we hypothesized that the various technologies involved in the preparation of protein rich ingredients could be directly responsible for the variation in their functional properties, such as interfacial and emulsification behaviour, which could be explained by their physicochemical properties. The overall aim of this study was to investigate the effects of different extraction methods on the structure–functionality relationship of PP and FBP isolates (PPI, FBPI) and concentrates (PPC, FBPC and deflavoured concentrates) along with appropriate controls from whey protein isolate (WPI) and egg white protein (EWP). Another objective was to develop an empirical model to predict emulsion properties based on protein characteristics. Although there are a great number of functionality studies involving pulse proteins in the literature, rarely do they directly compare the effect of extraction method on protein properties as well as functionality as an emulsifier in stabilizing oil-in-water (O/W) emulsions. The empirical model developed in this study may also be useful in identifying the relationship between protein ingredients, their characteristics and behaviour in emulsion systems.

2. Material and methods

2.1. Materials

The faba bean protein concentrate (product code: FBP60), deflavoured faba bean protein concentrate (DefFBP60), faba bean protein isolate (FBPI), pea protein concentrate (PP55), deflavoured pea protein concentrate (DefPP55), pea protein isolate (PPI), whey protein isolate (WPI), and pasteurized egg white protein (EWP) were donated by AGT Food Ingredients, Saskatoon, SK, Canada. The protein concentrates were produced by dry milling and air classification technology. Then, the obtained concentrates were hydrothermally treated to produce deflavoured concentrates according to proprietary processing technology. The protein isolates were produced by isoelectric precipitation technology. The WPI and EWP are standard conventional food emulsifiers widely used in the industry. Canola oil was purchased from a local supermarket at Saskatoon, SK, Canada. Milli-Q™ water (Millipore Corporation, Burlington, MA, USA) was used for the preparation of reagents for the protein assays and all other experiments. All acids and bases were obtained from Thermo Fisher (Edmonton, AB, Canada). All the other chemicals were purchased from Sigma Aldrich (Mississauga, ON, Canada).

2.2. Proximate analysis of protein powders

The proximate analysis of protein powders was done using AOAC and AOCS methods as follows: moisture: AOAC 925.09, protein: AOAC 992.15, ash: AOAC 923.03, starch: AOAC 996.11 and crude fibre: AOCS Ba 6a-06. Fat content was determined by the EPA 9071B-hexane extraction method, and carbohydrate content was determined by calculation.

2.3. Determination of protein solubility

For solubility, protein dispersions were prepared by dispersing 2 wt% of protein powders in deionized water and kept for stirring at 400 rpm overnight on a magnetic stirrer without pH adjustment and centrifuged at 6000 rpm for 30 min. The

supernatant was separated and used for measuring the protein content according to the method used by.[26] Freshly prepared biuret reagent was diluted eight times with 2.3% sodium bicarbonate, 4 ml of which was added to 1 ml of protein solution and held for 10 min at 25 °C. Next, 0.125 ml of 2 N Folin–Ciocalteu reagent was mixed, and the absorbance of the mixture was recorded immediately at 660 nm. Bovine serum albumin (BSA) was used as an internal standard for the protein content determination from the absorbance.[27] The protein solubility (% S) was calculated by eqn (1).

$$S(\%) = \frac{\text{the protein content of the soluble fraction}}{\text{the protein content of the whole powder}} \times 100 \quad (1)$$

2.4. Preparation and characterization of both soluble and insoluble fractions

2.4.1. Preparation of freeze-dried soluble and insoluble protein fraction. Protein dispersions (10 wt%) were prepared according to the method mentioned in Section 2.3. The dispersions were then centrifuged at 6000 rpm for 30 min at 25 °C. The supernatant was separately collected as soluble fraction. Both fractions were subjected to freeze-drying to prepare dried powder form of soluble and insoluble proteins for further analysis.

2.4.2. Determination of intrinsic fluorescence (IF) of soluble fractions. The freeze-dried soluble protein fraction was dispersed in deionized water at pH 7 at a concentration of 0.01 wt%. The protein dispersion was then used to determine its intrinsic fluorescence (IF) using a spectrofluorometer (FluroMax-4, Horiba Jobin Yvon Inc., Edison, N.J., USA). A constant excitation wavelength was maintained at 295 nm, and an emission range between 300 and 400 nm (increment of 1 nm) was used to determine the selective fluorescence spectra of aromatic amino acids.[28]

2.4.3. Fourier transform infrared spectroscopy (FTIR). Infrared spectra for freeze-dried soluble and insoluble protein fractions were recorded using a Renishaw Invia Reflex Raman microscope (Renishaw, Gloucestershire, UK) equipped with an IlluminatIR II FTIR microscope accessory (Smith's Detection, Danbury, CT). The absorbance at wavelengths from 4000 to 600 cm^{-1} was measured. Fourier self-deconvolution and second derivative analysis were performed in the amide-I region (1700–1600 cm^{-1}), and then the peaks were fitted to identify each secondary structure components using Renishaw's WiRE 3.3 software. Gaussian peaks could be assigned to their corresponding structure based on their peak position, and the integral of each peak was divided by the sum of all determined peaks to identify the proportion of each secondary structure.[29]

2.4.4. Protein composition using SDS-PAGE. Sodium dodecyl sulphate-polyacrylamide gel electrophoresis (SDS-PAGE) analysis was carried out to monitor the electrophoretic pattern of freeze-dried soluble and insoluble protein fractions. Samples containing 2 mg ml^{-1} of protein (30 μl) were mixed with 3 μl of NuPAGE® sample reducing agent (10×) and 7.5 μL of NuPAGE® LDS sample buffer (4×) (Invitrogen, Thermo Fisher Scientific, Carlsbad, CA) and finally, the volume was made up to 60 μl of deionized water. Aliquots of 15 μl were loaded onto the gel, and the separation was performed on 4–12% linear gradient polyacrylamide NuPAGE® Bis–Tris precast gels using a continuous buffer system (NuPAGE® MES SDS running buffer (1×), Invitrogen) for 60 min at a constant voltage supply of 200 V. The gels were removed from the cassettes and subjected for staining and de-staining process using rapid Coomassie protein SDS-gel staining protocol.[30] After staining & de-staining the gels, the pictures of gels were taken using a digital camera for further analysis.

2.5. Determination of protein powder functionality

2.5.1. Interfacial tension (IT) measurement. Interfacial tension (IT) of the protein dispersions against canola oil was measured using a Wilhelmy plate method *via* a K20 tensiometer (Kruss, Germany), operated at room temperature (25 ± 2 °C). A Wilhelmy plate was immersed 3 mm into 25 ml the 2 wt% aqueous protein dispersion after initial surface detection. Then, canola oil (40 ml) was pipetted gently into the cup on top of the aqueous phase, and the plate was raised 3 mm back to the original position. IT was calculated using the following equation.

$$\sigma = F/(\mathrm{L} \times \cos\theta) \quad (2)$$

where σ is the IT, F is the force detected by the force sensor, L is the wetted length of the plate, which is 40.20 mm, and θ is the contact angle between the aqueous phase and the plate. Since the plate was made of roughened platinum and it is optimally wetted, the contact angle would be 0. IT was recorded every minute for 30 minutes to obtain the values at equilibrium.

2.5.2. Determination of water (WHC) and oil holding capacities (OHC). Water (WHC) and oil holding capacity (OHC) were determined by suspending 0.5 g of protein powder in 5 g of water or oil in a 50 ml centrifuge tube. The dispersions were vortexed for 10 s every 5 min for a total of 30 min and then centrifuged at 5000 rpm for 15 min. The supernatant was carefully decanted, and the remaining pellet was weighed. Water/oil holding capacity was calculated by taking the ratio of weight gained by the protein samples to the initial sample weight. The water and oil holding capacities were expressed as g of water or oil per g of sample.[8]

2.5.3. Determination of zeta potential of protein dispersions. The 2 wt% protein dispersions were prepared in water by mixing them on a magnetic stirrer at 400 rpm overnight, followed by centrifugation at 6000 rpm for 30 min at room temperature. The supernatant was collected and adjusted to pH 2 and 7. The undiluted supernatant was then analyzed for its surface charge using a Zetasizer Nano-ZS90 (Malvern Instruments, Westborough, MA, USA).

2.6. Preparation of coarse emulsions using the protein powders and their characterization

2.6.1. Preparation of canola oil-in-water emulsions using pulse proteins. O/W emulsions were prepared at pH 2 and 7 by

dispersing 40 wt% canola oil in an aqueous phase containing 2 wt% protein powder, 0.25 wt% xanthan gum, and 0.02 wt% sodium azide (as an antimicrobial agent). By using similar powder concentration, we kept the total solid content in the emulsion constant, although they have different protein concentrations. This way, the effect of protein isolates and concentrates can be directly compared, and their influence on emulsion properties can be attributed to their composition. The pH of the aqueous phase was adjusted prior to mixing with the oil. The emulsion ingredients were mixed at a speed of 5000 rpm for 6 min using a rotor–stator blender (Polytron, Brinkman, ON, Canada). The freshly prepared O/W emulsions were stored at room temperature for further analysis.

2.6.2. Emulsion particle size analysis. The particle size distribution of the emulsions was measured using a static laser diffraction particle size analyzer (Mastersizer 2000, Malvern Instruments, Montreal, QC) immediately after their preparation and as a function of time (0 and 14 days) using deionized water as the dispersion medium. The volume-weighted mean droplet diameters ($D_{4,3}$) and the size distributions were recorded for further analysis.

2.6.3. Determination of surface charge of emulsions. Surface charge or zeta potential of the emulsions were determined using a Zetasizer Nano-ZS90 (Malvern Instruments, Westborough, MA, USA) by measuring the electrophoretic mobility (UE) of the oil droplets in an electric field. Three drops of emulsions were added to 50 ml deionized water at pH 2 & 7 prior to analysis. Zeta potential (ζ, mV) was measured as a function of time (0 and 14 days) for all emulsions.

2.6.4. Confocal laser scanning microscopy of emulsions. The confocal laser scanning micrographs of freshly prepared emulsions were taken with a Nikon C2 microscope (Nikon Inc., Mississauga, ON, Canada) using 543 and 633 nm lasers, a 60× Plan Apo VC (numerical aperture 1.4) oil immersion objective lens and 5 times digital zoom. All samples were prepared by adding 0.01 wt% Nile red (excitation by 543 nm laser, emission collected in 573–613 range) to the oil phase prior to emulsification and 0.01 wt% fast green (excitation by 633 nm laser, emission collected using a 650 nm long-pass filter) to the final emulsion to stain the proteins.

2.6.5. Viscosity and viscoelasticity of emulsions. The viscosity of the emulsions was determined using a rheometer (AR G2, TA Instruments, Montreal, QC, Canada) equipped with a 40 mm parallel plate cross-hatched geometer by keeping 1 mm gap as a function of shear rate in the range 0.01–100 s^{-1}. The viscosity was measured as a function of time (0 and 14 days) for all emulsions. Similarly, the viscoelasticity of the emulsions was measured by strain sweep analysis using the same instrument and geometry settings as in viscosity measurements. During the strain sweep test, the storage (G') and loss moduli (G'') were measured as a function of strain (0.01–1000%) at a constant frequency (6.28 rad s^{-1}).

2.6.6. Emulsion destabilization under accelerated gravitation. The long-term stability of the emulsions was determined using a photocentrifuge dispersion analyzer (LUMiSizer, LUM Americas, Boulder, CO, USA). Freshly prepared emulsions (400 μl) were transferred into 8 mm × 2 mm rectangular polycarbonate cuvettes and centrifuged at 4000 rpm (~2000 × g) for 16 h, during which transmission of an 865 nm laser through the sample was collected at 60 s interval. The transmission profiles were recorded by the SEPView software v 4.1 (LUM GmbH, Berlin, Germany), and percent emulsion destabilization was calculated from the length of the separated free oil region (lower transmission at the beginning of the profile) using the following equation:

$$\text{Destabilization}(\%) = \frac{\text{destabilized free oil phase height (mm)}}{\text{the total height of the sample (mm)}} \times 100 \quad (3)$$

2.6.7. Emulsion stability under different environmental stress conditions. The emulsions were subjected to different environmental stress conditions (addition of salt and heat treatment) in order to assess their stability in different food processing conditions. They were mixed with 1 wt% salt (NaCl), to match a typical salad dressing composition, and left overnight at ambient temperature before further analysis. For the heat treatment, the emulsions were kept at 90 °C for 30 min in a water bath and cooled to room temperature. The emulsions after salt addition and heat treatment were analyzed by determining their droplet size and charge.

2.7. Modeling

2.7.1. Evolutionary polynomial regression (EPR). Numerical regression is a powerful and commonly used form of regression to find the best fitting model for the experimental data sets.[31] EPR is a hybrid regression method that integrates the features of numerical regression with a multi-objective genetic algorithm.[32] The capability of the EPR to represent complex phenomena and experimental data has been proven in many application areas.[31,33–36] A general EPR expression can be written as eqn (4):[32]

$$Y = \sum_{j=1}^{n} \varphi\left(X, f(X), a_j\right) + a_0 \quad (4)$$

where Y is the vector of the output of the process, n is the maximum number of polynomial terms, φ is a function constructed by the process; a_j and a_0 are constants, X is a matrix of the input variables, and f is a user-defined class of function. In the current study, the EPR was used to derive three models for expressing the relation between emulsion characteristics (droplet size, destabilization and viscosity as responses, Y) and protein properties (such as solubility, intrinsic fluorescence, IT, WHC and OHC as variables, X). The EPR model class in eqn (5) was selected due to its low prediction error:

$$y = a_0 + \sum_{j=1}^{n} a_j \times (X_1)^{\mathrm{ES}(j,1)} \cdots (X_k)^{\mathrm{ES}(j,k)} \times f\left((X_1)^{\mathrm{ES}(j,k+1)} \cdots (X_k)^{\mathrm{ES}(j,2k)}\right) \quad (5)$$

where ES(j,z) is the exponent of the zth input within the jth term, and X_i is the candidate explanatory variables. The details

of the model can be found elsewhere.[32,37] The EPR-version 2.0SA toolbox, developed by Giustolisi and Savic,[32] was used to perform all the modelling runs.

Sensitivity analysis. The traditional and widely used one-factor-at-a-time (OFAT) approach[38] was used to investigate the strength of the relationship between the input and output parameters. In the OFAT approach, the effect of one independent factor on the dependent factor is monitored at a time, while other independent factors are fixed. The developed models using EPR were used to conduct OFAT analysis. The analysis was conducted by step by step, increasing one variable from its minimum to maximum value, while the other variables were kept fixed at their baseline values. Then, the selected variable was returned to its baseline value, and this procedure was repeated for the other inputs variables. For example, the effect of IT on the emulsion oil droplet size was analyzed by increasing the value of IT from its minimum to maximum while other factors (WHC, OHC, IF, *S*) were held constant at their mean values. This procedure was repeated for WHC, OHC, IF, *S* to investigate their effects on emulsion oil droplet size.

2.8. Statistical analysis

All measurements were done with three replications, and the results are reported as the mean ± one standard deviation. The experimental data were subjected to a general linear model or one-way analysis of variance (ANOVA). Data analysis was done using Minitab 19. Tukey's test was used to compare the mean values at $p < 0.05$ significance level.

3. Results and discussion

3.1. Effect of extraction method on structure–functional properties of faba bean and pea proteins

3.1.1. Proximate analysis. The moisture content of all protein samples varied from 3.9 to 7.2% (Table 1). Among the faba bean samples, FBPI had the highest protein content (87.0%), followed by DefFBP60 (60.5%) and FBP60 (57.6%). For pea, PPI had 80.6% while PP55 and DefPP55 showed 51.4 and 50.5% protein, respectively. The efficiency of air classification in separating starch from the protein fractions was shown to be low,[39] which explains the lower protein content of the concentrates (PP55 and FBP60). Karaca *et al.*[6] reported protein content of 84.1% and 88.8% for FBPI and PPI extracted *via* isoelectric participation, which was in a similar range to the values reported in the present case. In the case of fat content, the de-flavoured concentrate of both proteins had higher values (2.5% for DefPP55 and 2.1% for DefFB60) than the others. Among the plant proteins, the lowest fat content was observed for PPI and FBPI. Removal of fat prior to protein isolation led to higher protein content as the lipid–protein interactions limit the amount of extractable proteins.[40]

All pulse protein samples, except FBPI, had 5.2–5.4% ash. This was in agreement with Shand *et al.*,[41] who reported 5–5.9% ash in native and commercial PPI. FBPI had 9.0% ash, which can be due to its extraction by isoelectric precipitation, where the addition of alkali or acids could lead to the formation of salts and an increase in ash content. The lower ash content of PPI compared to FBPI might be due to the origin of proteins. The ash content of WPI was 0.6%, which was the lowest among all samples, and EWP had a slightly higher amount of ash (5.7%) than most of the pulse proteins. Among the pulse proteins, FBPI did not show the detectable amount of carbohydrates, and PPI had only 8%; however, the concentrates, PP55 and FBP60, had 34.3 and 29.2% of carbohydrates, respectively. The higher carbohydrate content of protein concentrates is well known, and it was due to the poor separation between the proteins and the carbohydrates by the dry fractionation process.

3.1.2. Protein solubility. All the pulse proteins showed significantly lower solubility compared to WPI and EWP, which were almost completely soluble ($p < 0.05$) (Fig. 1). Among the pulse proteins, FBPs (concentrates and de-flavoured) were more soluble than PPs obtained *via* dry fractionation and hydrothermal treatments. FBP60 had the highest solubility (69.9%), followed by DefFBP60, PP55, and DefPP55 with 50.2 and 46.2 and 44.0%, respectively. Both FBPI and PPI possessed significantly lower solubility compared to other protein fractions. Between the two isolates, FBPI (8.3%) was less soluble than PPI (20.5%). These differences could be the effect of processing conditions on proteins. The protein isolates were prepared with acid and alkali treatments, while the de-flavoured concentrates were processed with heat in the presence of water. Ma *et al.*[13] found a reduction in protein solubility due to boiling (wet heating) and roasting (dry heated) compared to untreated pulse flours. These can be due to the biochemical changes in protein structure, such as the cross-linking of proteins with starch and the formation of insoluble aggregates.[42] In addition, during processing, both hydrogen and non-polar bonds can lead to

Table 1 Proximate analysis of different pulse proteins samples[a]

Analysis (% w/w)	FBP60	DefFBP60	FBPI	PP55	DefPP55	PPI	WPI	EWP
Moisture	6.2	4.8	3.9	6.8	4.6	5.4	6.7	6.4
Protein	57.6	60.5	87.0	51.4	50.5	80.6	86.8	83.5
Lipid	1.6	2.1	0.04	2.1	2.5	0.8	0.03	0.4
Ash	5.4	5.4	9.0	5.4	5.3	5.2	0.6	5.7
Carbohydrates	29.2	27.2	n.d.	34.3	37.1	8.0	5.8	4.0
Total	100	100	100	100	100	100	100	100

[a] FBP60: faba bean protein concentrate, DefFBP60: de-flavoured faba bean protein concentrate, FBPI: faba bean protein isolate, PP55: pea protein concentrate, DefPP55: de-flavoured pea bean protein concentrate, PPI: pea protein isolate, WPI: whey protein isolate, and EWP: egg white proteins.

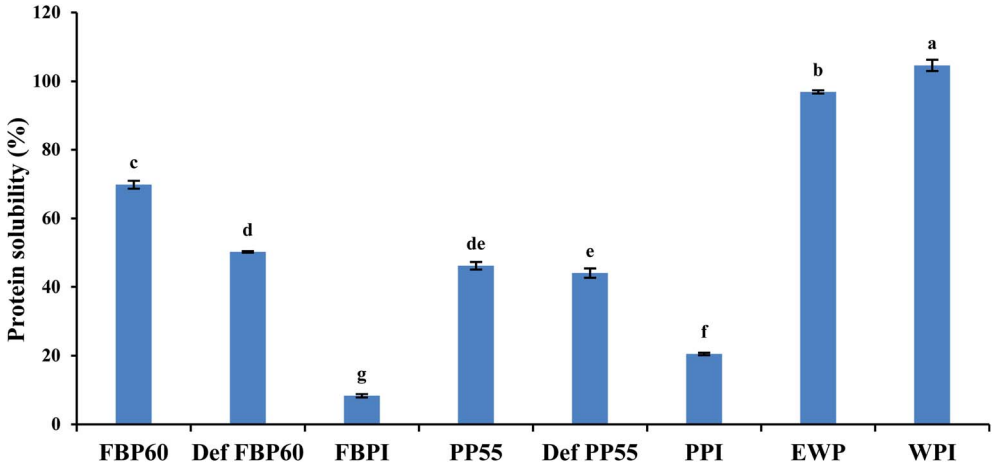

Fig. 1 Percent solubility of 2 wt% dispersions of different commercial pulse proteins samples in comparison with WPI and EWP. Means that do not share a letter are significantly different by Tukey's test at $p < 0.05$ significance level. See Table 1 for sample identification.

conformational changes in protein structure, leading to denaturation and lowering of solubility.[13]

3.2. Characterization of soluble and insoluble fractions

3.2.1. SDS-PAGE profiles of different protein samples. To confirm whether different processing methods influenced protein composition, SDS-PAGE was performed on both soluble and insoluble fractions of all samples (Fig. 2). The SDS-PAGE profiles are similar to the published results for WPI,[43] EWP,[44] FBP and PP.[45] Results from SDS-PAGE for pulse proteins showed thin bands of basic (19–22 kDa) and acidic (38–40 kDa) legumin (α and β) subunits. Separate bands for vicilin subunits (47–50 kDa) could also be observed.[28,45]

Both pea and faba bean showed high molecular weight proteins in the soluble fraction, probably due to the presence of polypeptide aggregates. For both the faba (FBP60) and pea concentrates (PP55), the soluble fraction had more faint bands at around 28 kDa, over 95 kDa and 250 kDa than the insoluble fraction; however, the intensity of the bands at ~40, 55, ~70, and 100 kDa was much higher in the insoluble fraction. For the

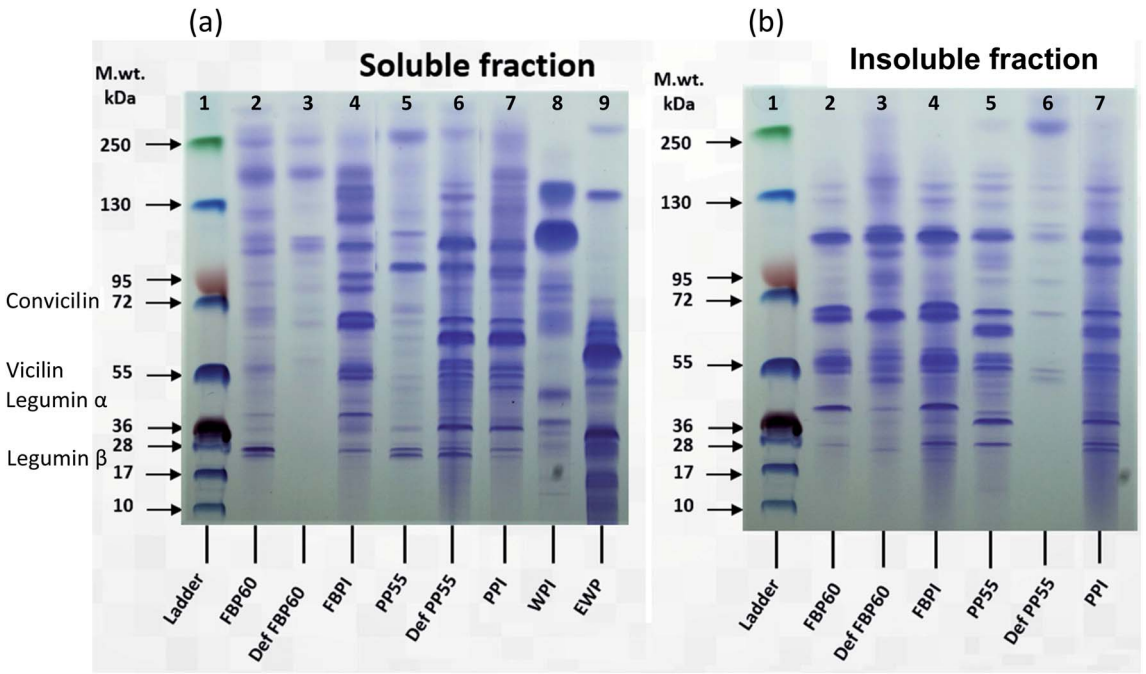

Fig. 2 (a) Soluble and (b) insoluble protein composition of different commercial protein samples by SDS-PAGE. The bands in lane 1 show the molecular weight of (MW) marker, ranging from 10 to 250 kDa. Lanes 2–4 in both (a) and (b) show results for different faba bean protein samples and lanes 5–7 for the pea protein samples. WPI and EWP (lanes 8 and 9, respectively) are only present in soluble fractions as they were completely soluble.

de-flavoured samples, a large difference can be seen between FBP and PP. The soluble fraction of DefFBP60 showed only a few faint bands higher than 95 kDa, but the insoluble fraction had higher intensity bands with a pattern similar to the insoluble fraction of FBP60, which indicates that the hydrothermal processing used for de-flavouring made the sample richer in insoluble fractions. In the case of DefPP55, however, several bands were observed (17–130 kDa) for the soluble fraction, while the insoluble fraction showed only a few weak bands. FBPI showed similar bands for MW of <72 for soluble and insoluble fractions but for higher MW bands (>95 kDa), the soluble fraction had a range of polypeptides up until 250 kDa, while the insoluble fraction showed a strong band at around 110 kDa and a few minor ones beyond 130 kDa. PPI, on the other hand, had almost the same pattern for both fractions.

DefFBP60 did not have any low molecular weight proteins in the soluble fraction, which can be caused by heating, while the opposite was true for DefPP55. Sorghum proteins were shown to have less intense bands in the cooked samples than the uncooked ones.[46] The authors suggested that his effect can be related to the decrease of extractability or formation of high molecular weight aggregates. In another study on the effect of high-temperature extrusion on the SDS-PAGE pattern of navy and pinto bean proteins, unlike albumin fractions (>40 kDa), extrusion temperature of 110 °C did not change the SDS-PAGE patterns of globulins. However, higher temperatures (135 and 150 °C) led to decreased intensity and disappearance of bands in the high MW region for both fractions, which was explained by their depolymerization during extrusion.[47]

Among the FBPs, the intensity of bands in both fractions was higher in FBPI than FBP60 and DefFBP60, which can be due to the higher protein content of the former. For PPs, among the soluble fractions, DefPP55 and PPI had similar patterns, but PP55 showed less intense bands. Among the insoluble fraction, PP55 and PPI had a similar pattern; however, DefPP55 showed bands with much lower intensity. PPI in both fractions had more intense bands than the two other PP types, which could be due to its higher protein content.

3.2.2. Secondary structures of various pulse protein samples. During processing, the application of heat, addition of acid/alkali, or salt could influence protein's secondary structure, which could explain their functionality, such as solubility and emulsification behaviour. Previously, the β-sheet was reported as the most significant structure in the raw bean. In thermally dried beans, α-helix was disappeared entirely, and a significant decrease was observed for the β-sheet.[29] In autoclaved samples, random coil (RC) and aggregates ($A_1 + A_2$) were the most common structure.[29] Here, we also looked at the secondary structure of both soluble and insoluble fractions of each pulse protein samples to find out if any particular secondary structure components dominate in either fraction.

In almost all of the samples, inter-molecular aggregates (A_1) were the most dominant secondary structure, followed by a β-sheet and random coil (Fig. 3). Intramolecular hydrogen bonds are the weakest, which could be the reason behind the lower α-helix compared to the β-sheet. The alkaline condition used for PPI and FBPI production decreased β-sheet and RC except for the insoluble fraction of PPI. Similarly, Law *et al.*[48] observed a decrease in the α-helix and β-sheet content of *Dolichos lablab* vicilins in extreme alkaline conditions.[48] Both the soluble and insoluble fractions of hydrothermally treated DefFBP60 showed significantly higher random coil and β-sheet structure and significantly lower inter-molecular aggregates compared to the other two FBP samples. Reorganization of the protein secondary structure was also observed after the heating of protein isolate of kidney bean.[49] Between the soluble and insoluble fractions of FBP, the only difference in secondary structure could be seen in β-sheet and inter-molecular aggregates, which was lower in the soluble fractions compared to the insoluble fractions. Among the three different pea samples, almost no difference in secondary structure could be seen in the insoluble fractions. In the soluble PP, the de-flavoured sample had more β-turn and less α-helix compared to the other two, and the isolate had significantly higher inter-molecular aggregates. Between the soluble and insoluble fractions of PP, soluble fractions had more inter-molecular aggregates and random coils in both the concentrates and lower α-helix in the de-flavoured concentrate. For isolates, there was no significant difference between the soluble and insoluble fractions.

We initially hypothesized that the soluble fractions could have fewer aggregates and β-sheet due to the predominant hydrophobic nature of these two structures and more random coils due to the possibility of better dispersion in the aqueous phase. Also, there could be differences in the secondary structure based on the different processing methods for the concentrates, de-flavoured concentrates and isolates. However, except for a few samples mentioned above, not much consistent difference in secondary structure can be seen among the various samples and their soluble and insoluble fractions. Therefore, the secondary structure of protein identified using FTIR cannot be used as a good indicator of their solubility and functionality. Perhaps, the tertiary structure of protein could be a better indicator.[50]

3.2.3. Intrinsic fluorescence of various pulse protein samples. The structural and environmental changes in the aromatic amino acids (phenylalanine, tyrosine and tryptophan) of protein influence its fluorescence spectra. Therefore, the intrinsic fluorescence of the protein solutions was captured to understand the relative changes in protein tertiary structure based on processing conditions and solubility (Fig. 4a). All the pulse protein samples showed much higher fluorescence intensity in their soluble fractions compared to the insoluble fractions, which indicates the presence of more aromatic amino acids. Otherwise, it is also possible that the hydrophobic aromatic amino acids were less exposed to the aqueous phase in the soluble fractions due to the changes in protein conformation to hide them, leading to less quenching and hence higher signal intensity. For the soluble fractions, there was no significant difference between pea and faba bean samples under similar processing conditions. The soluble fractions of DefFBP60 and DefPP55 showed lower fluorescence than their corresponding concentrate and isolates, which could be due to the hydrothermal treatment of the proteins during processing

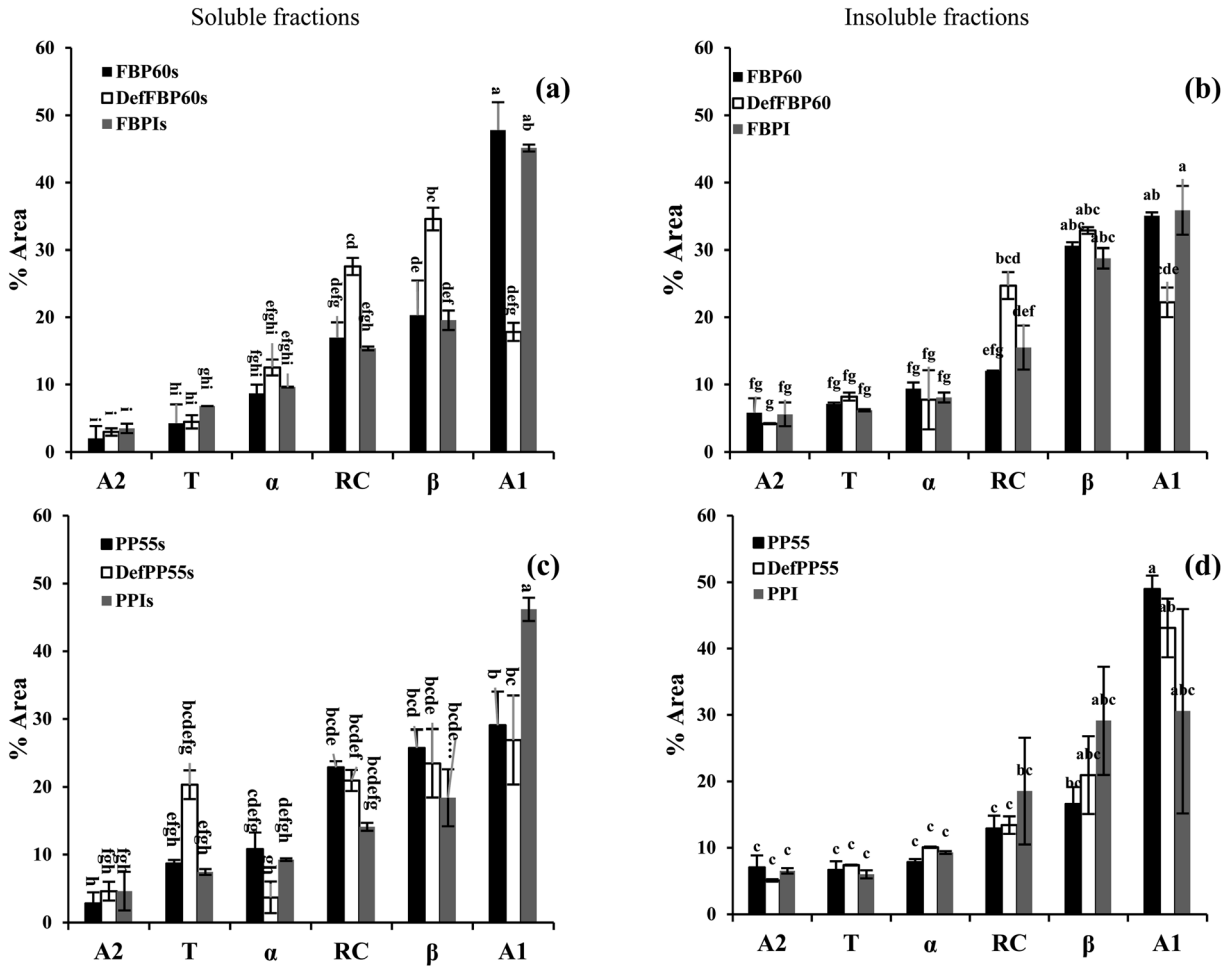

Fig. 3 Contribution from different secondary structure components of different commercial pulse proteins samples using FTIR. Faba bean proteins ((a) soluble and (b) insoluble fraction), pea proteins ((c) soluble and (d) insoluble fraction). A2: intra-molecular aggregate, T: beta-turn, α: alfa-helix, RC: random coil, β: beta-sheet, and A1: inter-molecular aggregate. Means that do not share a letter are significantly different by Tukey's test at $p < 0.05$ significance level. See Table 1 for sample identification.

leading to higher quenching or loss of some aromatic amino acids.

3.3. Determination of protein powder functionality

3.3.1. Interfacial tension. All the proteins used in this research showed significantly lower IT than the pure oil–water interface ($p < 0.05$), indicating surface activity and possible emulsifying ability (Fig. 4b). All samples from faba bean and EWP had higher IT at pH 2 than pH 7, while samples from PP and WPI showed similar IT at both the pH values. In contrast, Chang *et al.*[51] observed higher IT at pH 3 compared to pH 7 for PPI (12 and 9 mN m^{-1}, respectively). At pH 2, there was not much difference in IT among the various samples; however, at pH 7, IT of all FBP and EWP was significantly lower than all PP and WPI ($p < 0.05$). The lowest IT belonged to EWP at pH 7 (6.7 mN m^{-1}), followed by FBP60, FBPI and DefFBP60 at pH 7 (7.0, 8.0 and 8.5 mN m^{-1}, respectively). There was no apparent difference among the concentrate, de-flavoured or isolate forms at a particular pH. The IT of different protein concentrations and oil types were reported to be 24 mN m^{-1} for 0.04 wt% PPI at pH 7 against medium-chain triglyceride,[52] 42 mN m^{-1} for 0.25 wt% FBPI and PPI at pH 7 against flaxseed oil,[6] 8 mN m^{-1} for 0.1 wt% FBPI at pH 7 against canola oil,[53] and 26 mN m^{-1} for 0.3 wt% PP at pH 7 against soybean oil.[25] Such a wide range of values reported in literature could be attributed to sources and concentration of pulse proteins, dispersion pH, oil impurity (such as monoglyceride) and the methods used for IT determination.

3.3.2. Water and oil holding capacity. At both pH 2 and pH 7, the isolates (FBPI and PPI) had the highest WHC, followed by their de-flavoured and concentrate forms (Fig. 4c). In a study on field peas and faba bean, similar to our results, protein isolate showed higher water and oil holding capacities than concentrates.[39] The higher WHC of the protein isolates has been attributed to their higher protein content and smaller starch fragments.[10] WHC of PPC reported by Toews & Wang[54] was found to be similar to the values reported here. Between the two pH values, for both the concentrates (FBP60, PP55) and the de-flavoured concentrates (DefFBP60 and DefPP55), WHC at pH 2 was higher than pH 7. Contrastingly, for the isolates, WHC at

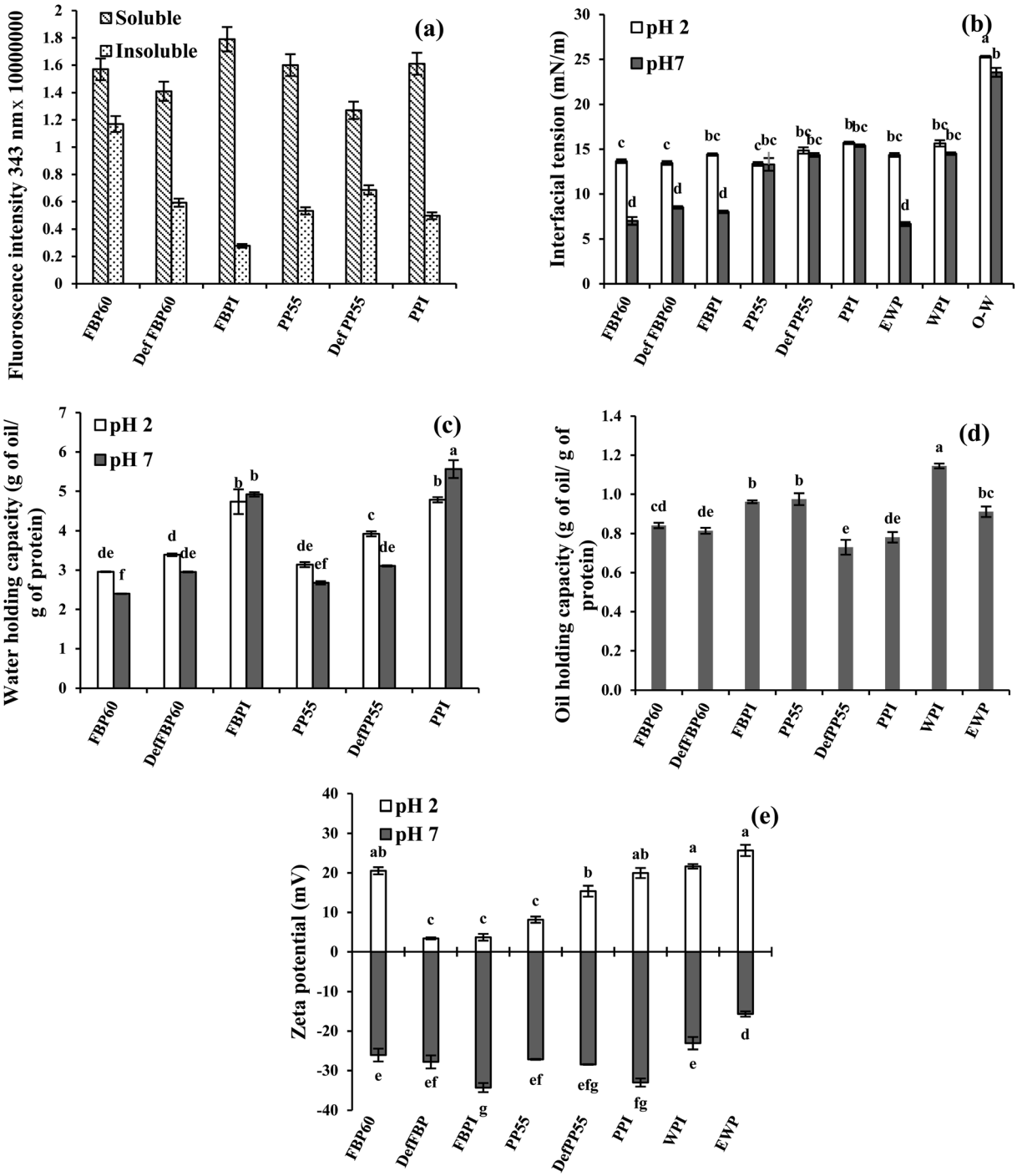

Fig. 4 (a) Effect of processing conditions on intrinsic fluorescence of soluble and insoluble proteins fraction; (b) canola oil–water interfacial tension; (c) water holding capacities; (d) oil binding capacities; and (e) zeta potential of 2 wt% dispersions of various commercial pulse proteins samples at pH 2 and pH 7. Means that do not share a letter are significantly different by Tukey's test at $p < 0.05$ significance level. See Table 1 for sample identification.

pH 7 was higher compared to pH 2 for PPI and not significantly different for FBPI. WHC was not reported for WPI and EWP, as they were completely dissolved in water at both pH values and not suitable for water holding.

WHC can also be affected by protein conformational and environmental factors,[55] and the processing used for protein extraction. Stone *et al.*[8] reported that at pH 7, micellar precipitated (MP) PPI had higher WHC (3.2–3.6 g g^{-1}) than alkali extraction-isoelectric precipitated (AE-IP), and SE-dialyzed PPI (2.4–2.6 and 0.34–2.6 g g^{-1}, respectively). The higher WHC in MP PPI was ascribed to the higher exposure of polar groups and side-chain amino acids of proteins to water and the formation

of more hydrogen bonds, while in AE-IP PPI, the protein structure was disturbed, leading to their lower ability to interact with water. In the present case, the WHC of the isolates (AE-IP) was highest among the various samples, and the values were higher than that reported by Stone *et al.*,[8] which could be due to the difference in origin of the proteins samples and processing used for the extraction.

Among the various proteins, oil holding capacity (OHC) was highest for WPI (1.15 g oil per g of protein), followed by PP55, FBPI and EWP (0.97, 0.96 and 0.91 g g^{-1}, respectively) (Fig. 4d). There was no particular trend in OHC of the pea and FBPs samples. For example, in FBPs, the isolate showed the highest OHC followed by similar values for concentrate and de-flavoured samples, while in PPs, concentrate showed the highest OHC, followed by similar values for de-flavoured and isolate samples. OHC of unheated PPC was reported to be 1.28 g g^{-1} (23). Stone *et al.*[8] reported an OHC of 5.2–5.4 g g^{-1} for SE PPI, while AE-IP and MP showed lower values (3.5–3.8 g g^{-1} and 3.6–3.7 g g^{-1}, respectively), which might be a result of different surface properties of the proteins. The researchers also obtained higher OHC for egg (2 g g^{-1}) and whey proteins (1.4 g g^{-1}) compared to the present study. OHC is a result of physical entrapment of oil in the protein structure; thus, it can be affected by protein type, concentration, charge, hydrophobicity, surface area and size of the protein.

3.3.3. Zeta potential of protein dispersions. For all samples, the zeta potential was positive at pH 2 and negative at pH 7 (Fig. 4e). It is well known that the isoelectric point (pI) of pulse proteins is between pH 4 to 5.[56] For WPI, pI is 4.5.[57] The pI of the major component of EWP was also reported to be around pH 4.5.[58] At pH 7, for both FBP and PP, the highest zeta potential was for the isolates followed by the de-flavoured samples and the concentrates, which could be due to the higher protein content of the isolates and the presence of polysaccharides in the concentrates that could partially neutralize the charges on protein molecules. FBPI had the highest zeta potential at −34.3 mV, followed by PPI at −33.0 mV. Zeta potential of PPI and FBPI obtained by the AE-IP technique was reported to be −43.5 mV at pH 7,[59] and −46.4 mV at pH 7,[53] respectively. On the other hand, Karaca *et al.*[6] reported the zeta potential of FBPI and PPI at pH 7 as −23 mV and −21 mV, respectively. Such a difference in zeta potential among the various researchers could be due to the origin of the proteins and the extraction process.

At pH 2, PP showed a similar trend as pH 7 with the highest zeta potential for the isolate (+19.9 mV) followed by the de-flavoured sample and the concentrate. However, for FBPs at pH 2, the zeta potential was highest for the concentrate (+20.5 mV), while it was significantly lower for the isolate (+3.7 mV) and the de-flavoured samples (+3.4 mV). Such a low zeta potential for the FBPI at pH 2 is surprising, considering its higher protein content and highest zeta potential at pH 7. FBPI had the highest mineral content (ash 9.0%), which could lead to more charge screening due to increased solubility of the minerals at acidic pH and corresponding lowering of zeta potential. The zeta potential of the pulse proteins was similar or lower than EWP and WPI at pH 2, while at pH 7, for all pulse proteins, it was higher than EWP, while they are similar to WPI (Fig. 4e).

3.4. Preparation of coarse emulsions using the protein powders and their characterization

3.4.1. Emulsion average particle size. The volume average particle sizes of the emulsions reported in Fig. 5a–d are actually the average of individual and aggregated oil droplets and protein particles, as the particle size analyzer does not distinguish between them. At pH 2, the particle size of all FBP-stabilized emulsions was significantly smaller compared to PP, WPI and EWP, indicating the superiority of faba proteins over all others under the specific emulsification conditions. It was previously shown that the FBP concentrates produced the smallest droplets compared to pea and lentil proteins.[60] At pH 2, however, the aggregate size of all emulsions was significantly higher compared to pH 7, which was more pronounced in the case of PP, WPI and EWP. The smaller IT of FBPs at pH 7 can lead to the formation of smaller emulsion droplets. This effect was also observed for EWP and WPI. For PP, however, in spite of IT at pH 7 being similar to pH 2 (Fig. 4b), particle size was much smaller at pH 7. Such an improved emulsification behaviour at pH 7 could be attributed to the higher zeta potential of PP at pH 7 compared to pH 2.

At pH 7, of all freshly prepared emulsions, WPI had the smallest (8.19 μm), while EWP had the highest (33.9 μm) average particle size. Among the pulse protein emulsions at pH 7, PP55 showed the smallest (8.6 μm), and FBPI showed the largest particle size (25.8 μm). For both FBP and PP, isolate-stabilized emulsions were formed with larger particle sizes compared to the concentrates or de-flavoured samples, although isolates had much protein content than the concentrates. This could be due to the denaturation of pulse proteins during isolate preparation leading to lower solubility (as shown in Fig. 1), which hindered the formation of smaller emulsion droplets and led to protein and oil droplet aggregation.

Effect of storage time. For all FBP samples, some increase in average particle size was observed after 14 days at pH 2, while at pH 7, no such change was observed upon storage (Fig. 5a and b). For PP at pH 2, no increase was observed; rather, some drop in average particle size was observed for PP55 and PPI, which could be attributed to the loss of large oil droplets due to emulsion destabilization. At pH 7, DefPP55 and PPI showed a noticeable increase in droplet size after 14 days, which can be due to droplet flocculation and protein aggregation, as also observed by Yerramilli *et al.*[28] At pH 2, WPI and EWP emulsions showed no change upon storage, while at pH 7, only EWP showed a significant decrease in size after 14 days.

Effect of heat treatment. At pH 2, all samples except DefFBP60 and FBPI emulsions showed phase separation after heat treatment, leaving a clear aqueous phase at the bottom of the glass vials (Fig. 6a). In contrast, at pH 7, none of the samples showed phase separation after heating (Fig. 6a), indicating improved visual stability. Heat treatment led to a particle size increase in all the pulse protein-stabilized emulsions at pH 7, while at pH 2, except PP, similar behaviour was observed for all FBP samples

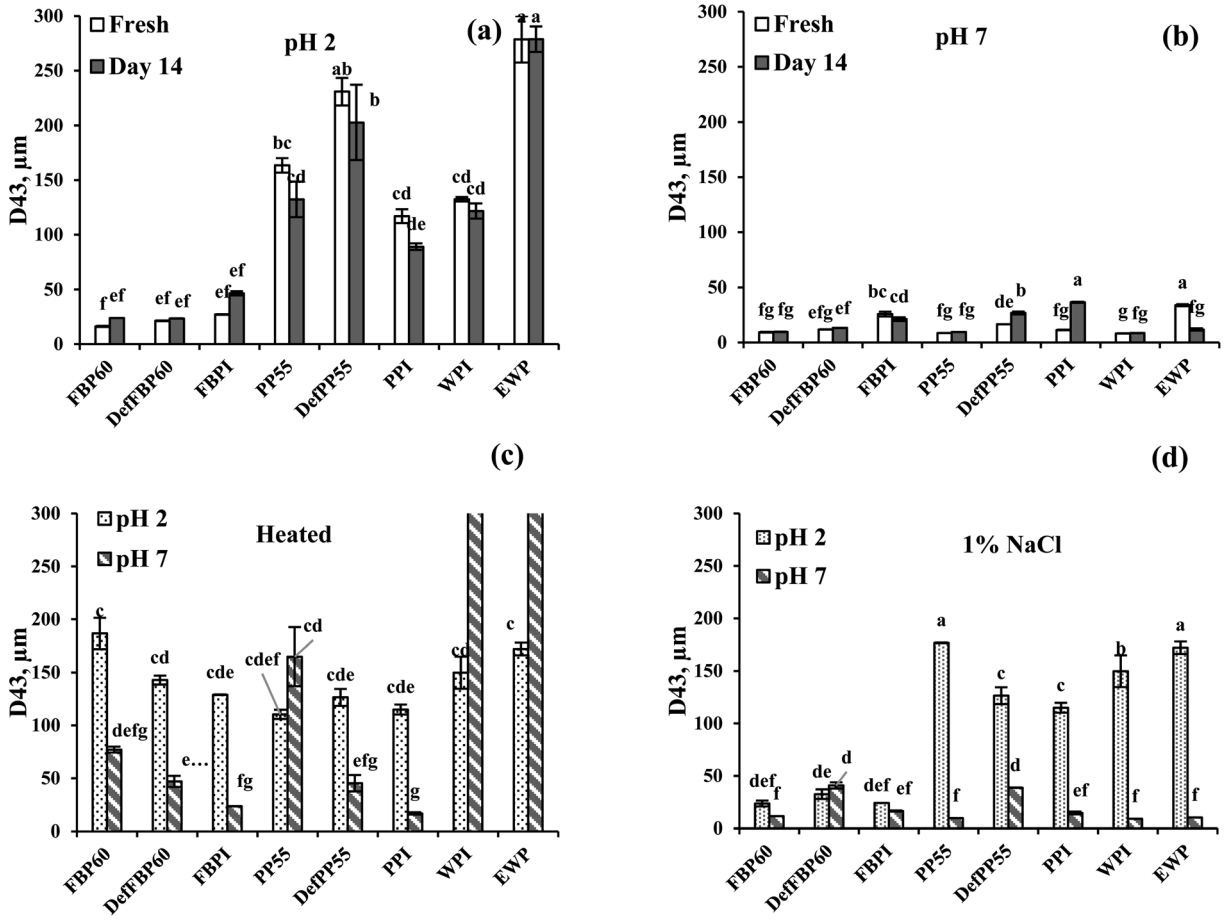

Fig. 5 Volume average droplet size ($D_{4,3}$) of emulsions prepared using different commercial pulse proteins samples. Droplet size of freshly prepared emulsions and as a function of storage time (day 7 and 14) is shown at (a) pH 2 and (b) pH 7. The effect of (c) heat treatment (90 °C for 30 min) and (d) the addition of 1 wt% salt on the average droplet size at pH 2 and pH 7 are also shown. Means that do not share a letter are significantly different by Tukey's test at $p < 0.05$ significance level. See Table 1 for sample identification.

(Fig. 5a *vs.* Fig. 5c). At pH 2, PPC55 and DefPP55 had smaller droplet size after heating, which could be due to the loss of very large oil droplets in the emulsions before heating. For PPI emulsion at pH 2, no change was observed upon heating. Partial destabilization of heated emulsions could be attributed to heat-induced protein denaturation leading to further aggregation in

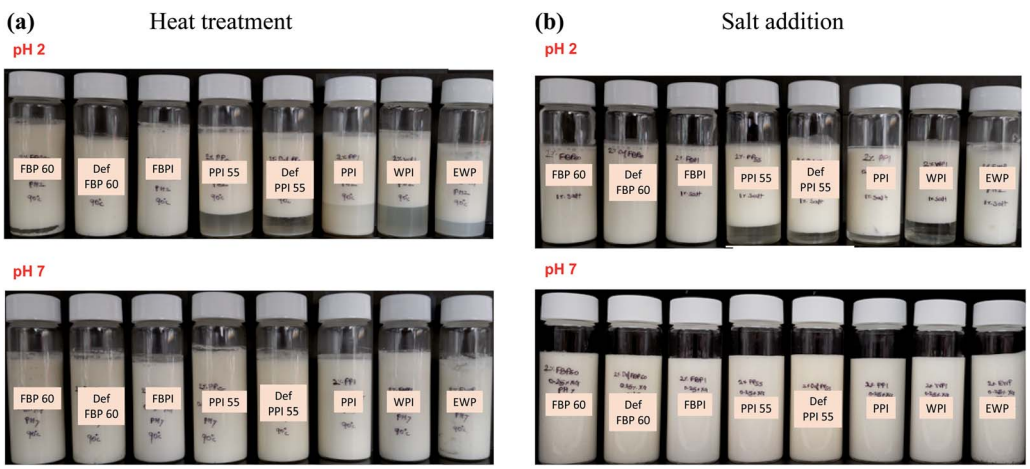

Fig. 6 Effect of (a) heat treatment (90 °C for 30 min), and (b) 1 wt% salt addition on the visual appearance of various commercial protein-stabilized emulsions at pH 2 and pH 7. See Table 1 for sample identification.

oil droplets and protein aggregates. Among the different samples from the same proteins, heat treatment led to a decreased particle size (probably due to loss of large oil droplets) from concentrate to isolate, except PP emulsions at pH 2. WPI and EWP emulsions showed no increase when heated at pH 2; however, a considerable size increase was observed from about 8.2 to 380 μm for WPI and from about 10 to 827 μm for EWP after heating at pH 7. This could be due to the heat-induced protein denaturation and related aggregation, which were more pronounced for WPI and EWP compared to pulse proteins. An increase in droplet size of 10 wt% algae O/W emulsions (pH 7) stabilized by FBP and PP was observed as the temperature was increased from 20 to 90 °C.[60]

Effect of salt. At pH 2, the addition of 1% NaCl led to visual phase separation in emulsions stabilized by all PP and WPI emulsions (Fig. 6b), which is in accordance with their larger particle size (Fig. 5d). For FBP emulsions, no separation was observed upon salt addition at pH 2, and the emulsion particle size also did not show any significant increase compared to the fresh ones (Fig. 5a *vs.* Fig. 5d). Salt addition also caused a significant particle size decrease in EWP emulsion at pH 2 (Fig. 5d), but no phase separation was observed (Fig. 6a). At pH 7, no phase separation was observed in any emulsions (Fig. 6b); however, an increase in particle size was observed for DefFBP60, DefPP55 and PPI-stabilized emulsions after salt addition. The particle size of all other emulsions at pH 7 remained stable even after salt addition (Fig. 5d). The addition of salt induces electrostatic charge screening, leading to droplet aggregation. However, a strong protein layer around the droplets may provide steric stabilization, which could prevent salt-induced droplet aggregation.[61] Moreover, excessing droplet aggregation due to the presence of salt may also lead to apparent stabilization of emulsion by creating a network of droplet aggregates that could prevent phase separation. For FBPs, emulsion stability was not affected by 1 wt% salt irrespective of pH, which could be important for its application in food. A similar increase in mean particle size was observed for soy protein isolate-stabilized emulsions at an intermediate ionic strength (100 mM NaCl).[62] However, the authors noted increased emulsion stability at a higher salt concentration (400 mM NaCl), which was ascribed to the salting-in effect of proteins. Our salt concentration was around 160 mM, which probably would not provide a salting-in effect, but depending on the aggregate size, phase separation could be prevented. The influence of pH and NaCl on the structure of globulin protein was studied by Castellani *et al.*[63] Their results showed that the protein was stable at pH 5 to 9 but by decreasing pH below 5 was rapidly unfolded, which could lead to aggregation of protein coated droplets. The author also proposed that increase in NaCl concentration above 100 mM increased the protein denaturation temperature and enthalpy, thereby making the protein more stable. In the present case, such increase in protein stability in the presence of salt could also be responsible for emulsion stability.

3.4.2. Emulsion zeta potential

Effect of pH. Similar to the proteins in Fig. 4, most emulsions carried a positive zeta potential at pH 2, which is lower than the isoelectric point (pI) of the proteins (Fig. 7a). This is also in accordance with other studies on legume proteins.[60] The only exception to this was the emulsion stabilized by FBPI, which had a slight negative zeta potential (-4.9 ± 0.6 mV). For all other emulsions, droplet charge varied from -28.9 ± 1.8 (for WPI) to -36.1 ± 3.1 mV (for PP55). The different behaviour of FBPI can be related to its ash content, which was almost two times more than other samples (Table 1). The presence of a high concentration of mineral salts can lead to salt-induced charge screening and a drop in zeta potential, which could even lead to charge reversal due to the salting-in effect.[62] At pH 7 (higher than pI) all emulsions carried a high negative zeta potential ranged from -48.1 ± 0.5 (EWP) to -68.7 ± 2.0 mV (FBPI) (Fig. 7b). Higher zeta potential provides more electrostatic repulsive force and, consequently, more emulsion stability. This agrees with the results of droplet size measurement where at pH 7, with greater zeta potential, smaller particles were obtained compared to pH 2 (Fig. 5a). Interestingly, the zeta potential of emulsions was much higher compared to the corresponding protein dispersions, as reported in Fig. 4e. For example, the zeta potential of all pulse proteins stabilized emulsions at pH 7 increased from around -30 mv for protein dispersion to more than -60 mV for emulsions. Also, at pH 2, the zeta potential of protein dispersions was <26 mV, but emulsions showed >28 mV. Such an increase in zeta potential upon proteins' adsorption at the oil droplet surface has been reported by others and was attributed to surface denaturation of proteins leading to more exposure of the ionic groups towards the aqueous phase.[64] After 14 days of storage, the zeta potential of all emulsions at pH 2 and 7 stayed unchanged (Fig. 7a and b).

Effect of heat treatment. For most of the pulse protein-stabilized emulsions, heat treatment showed a decrease in zeta potential, which could be attributed to heat-induced protein denaturation leading to protein and oil droplet aggregation (Fig. 7c). A more substantial drop in emulsion zeta potential was observed at pH 2 compared to pH 7, which shows that the proteins were more susceptible to denaturation under acidic conditions. The most significant drop in zeta potential was observed for FBP60 and DefFBP60 at pH 2, followed by PP55 and DefPP55. For FBPI emulsion at pH 2, zeta potential reached zero from -4.9 mV after the heat treatment. PPI, on the other hand, showed a minimum decrease in emulsion zeta potential compared to the untreated samples at pH 2. WPI showed a slight decrease, while EWP showed an insignificant increase in emulsion zeta potential upon heating. At pH 7, FBP-stabilized emulsions did not show a significant change in zeta potential before and after heat treatment. PP and WPI-stabilized emulsions, however, showed a slight decrease in zeta potential, while EWP showed an increase in zeta potential upon heat treatment. In accordance to our results, Gumus *et al.*[60] also reported a decrease in the magnitude of the zeta potential of PP and FBP-stabilized emulsions by heating above the thermal denaturation temperature of proteins and proposed that conformational changes in proteins upon heating changed the exposure of charged groups or the number of bound counter-ions.

Effect of salt. As expected, in all emulsions, salt addition caused a dramatic decrease in zeta potential due to the charge screening effect (Fig. 7d). Similar to heat treatment, a more

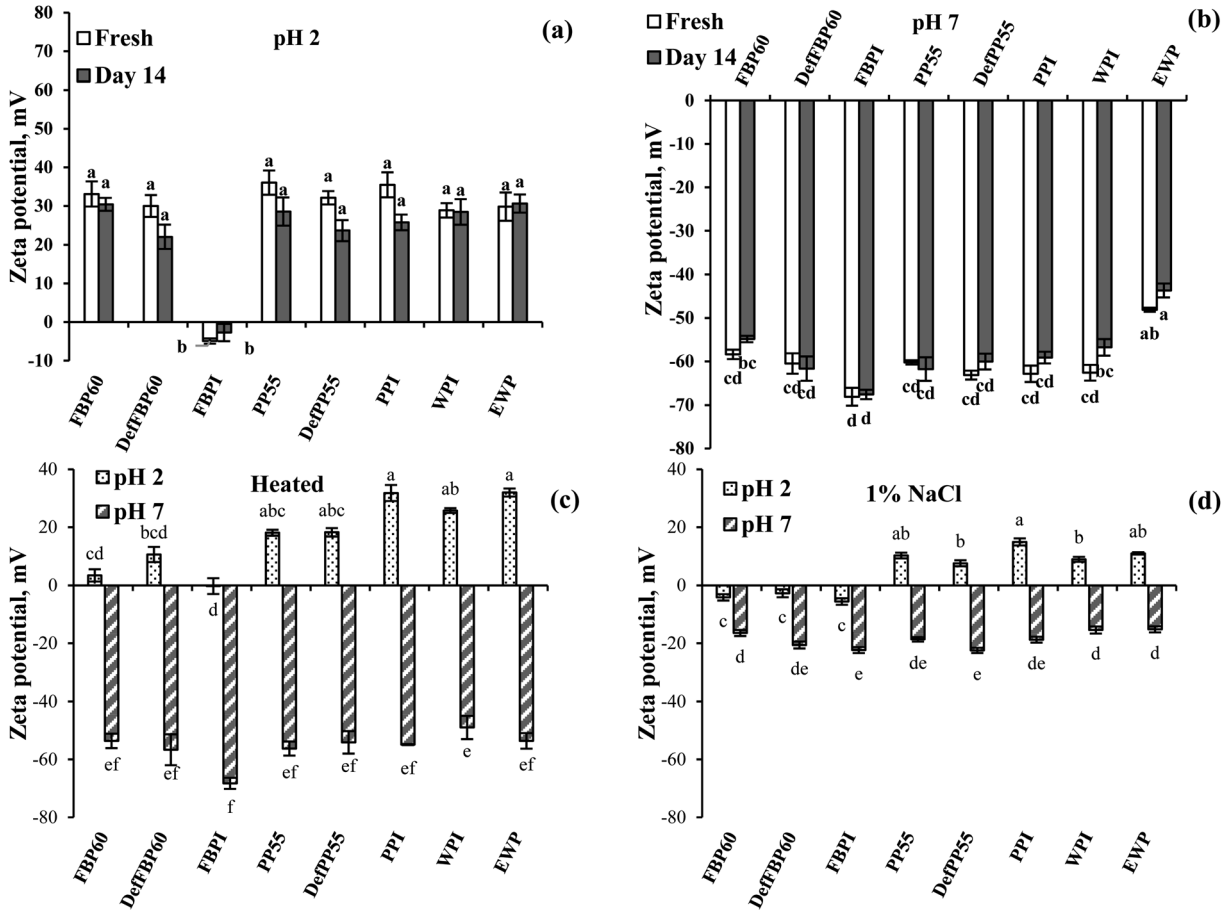

Fig. 7 Effect of storage time on zeta potential of emulsions prepared using various commercial protein samples (a) at pH 2 and (b) at pH 7, (c) effect of heat treatment (90 °C for 30 min) and (d) effect of 1 wt% salt addition as a function of pH. Means that do not share a letter are significantly different by Tukey's test at $p < 0.05$ significance level. See Table 1 for sample identification.

significant drop in zeta potential was observed at pH 2 compared to pH 7. For example, at pH 2, salt addition decreased the zeta potential for PP, WPI and EWP emulsions from nearly 30 mV to 7–15 mV. For FBP60 and DefFBP60-stabilized emulsions at pH 2, salt addition even changed zeta potential from high positive to very low negative values (−2.7 to −5.6 mV). However, these low values of zeta potential at pH 2 did not show a significant increase in emulsion aggregate size, which could be attributed to the steric stabilization effect, as discussed above. At pH 7, the zeta potential of emulsions dropped to around −20 mV from −60 to −70 mV before salt addition; however, −20 mV was enough to keep the droplets from aggregation, such that the emulsions remained stable without any significant increase in particle size or change in visual observation. Similar to our data, the addition of NaCl (500 mM) to PP and FBP-stabilized emulsions at pH 7 was also reported to decrease the magnitude of zeta potential from −18 and −17 mV to −8 mV, respectively.[60]

3.4.3. Emulsion microstructure. The confocal laser scanning micrographs of all emulsions showed spherical oil droplets (in red) and protein aggregates (in green) in the continuous phase (Fig. 8). At pH 2, FBP-stabilized emulsions had smaller droplets compared to PP-stabilized emulsions, which confirms the results for particle size measurement (Fig. 5a). From the results of confocal microscopy, it appears that the PP-stabilized emulsions at pH 2 were not quite suitable for further application as the presence of irregular and more extensive oil phase indicates emulsion destabilization. WPI and EWP also showed large oil droplets at pH 2, but their oil droplets remained spherical shape, which indicates better emulsion formation than PP. Numerous smaller oil droplets were observed at pH 7 compared to pH 2 for all protein samples, which confirmed the particle size data reported in Fig. 5a and b, indicating superior emulsion stability.

3.4.4. Emulsion rheology

Apparent viscosity. All the emulsions prepared showed shear-thinning behaviour where viscosity decreased as a function of shear rate (data not shown). To better compare the viscosity of different emulsions, the apparent viscosities at 1 s^{-1} shear rate was plotted as a function of storage time at pH 2 and pH 7 (Fig. 9). At pH 2, FBP-stabilized emulsions showed the highest apparent viscosities (~6 Pa s) followed by EWP (~2.5 Pa s), while the viscosities of PP and WPI-stabilized emulsions were very low (Fig. 9a). The apparent viscosities of all emulsions stabilized with PP were significantly lower than FBP, which could be attributed to the larger oil droplets and higher emulsion

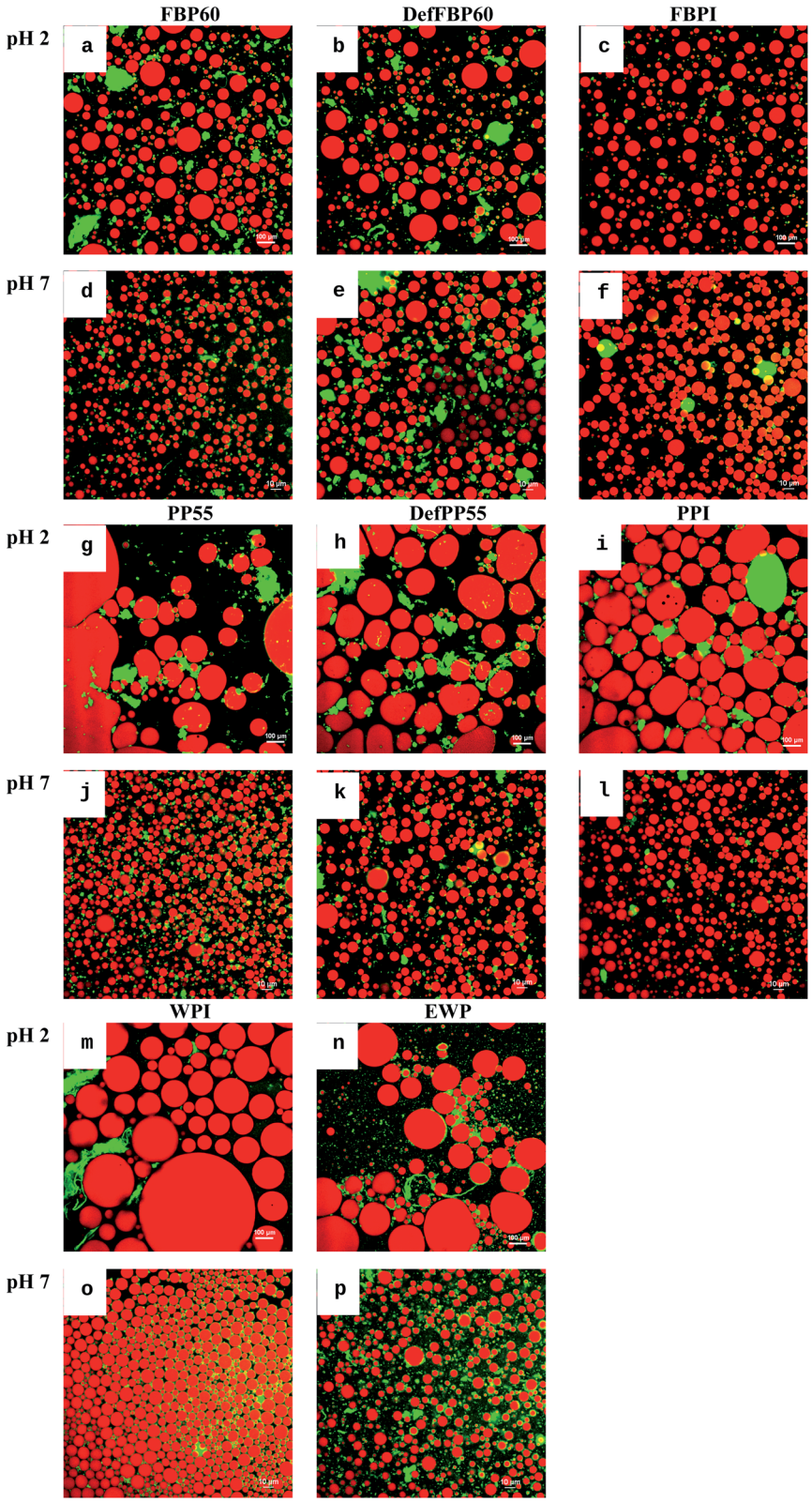

Fig. 8 Confocal laser scanning micrographs of oil-in-water emulsions prepared using various commercial protein sample. (a–f) Faba bean proteins, (g–l) pea proteins, (m and n) WPI and (o and p) EWP at pH 2 and pH 7. Scale bar represents 10 μm. See Table 1 for sample identification.

destabilization in the former. At pH 7, apparent viscosities of most emulsions significantly increased compared to pH 2, except for FBP60 and DefFBP60, where viscosity remained unchanged. The effect of pH on viscosity was more noticeable for PP-stabilized emulsions. The smaller droplet size of PP-stabilized emulsions at pH 7 was probably responsible for

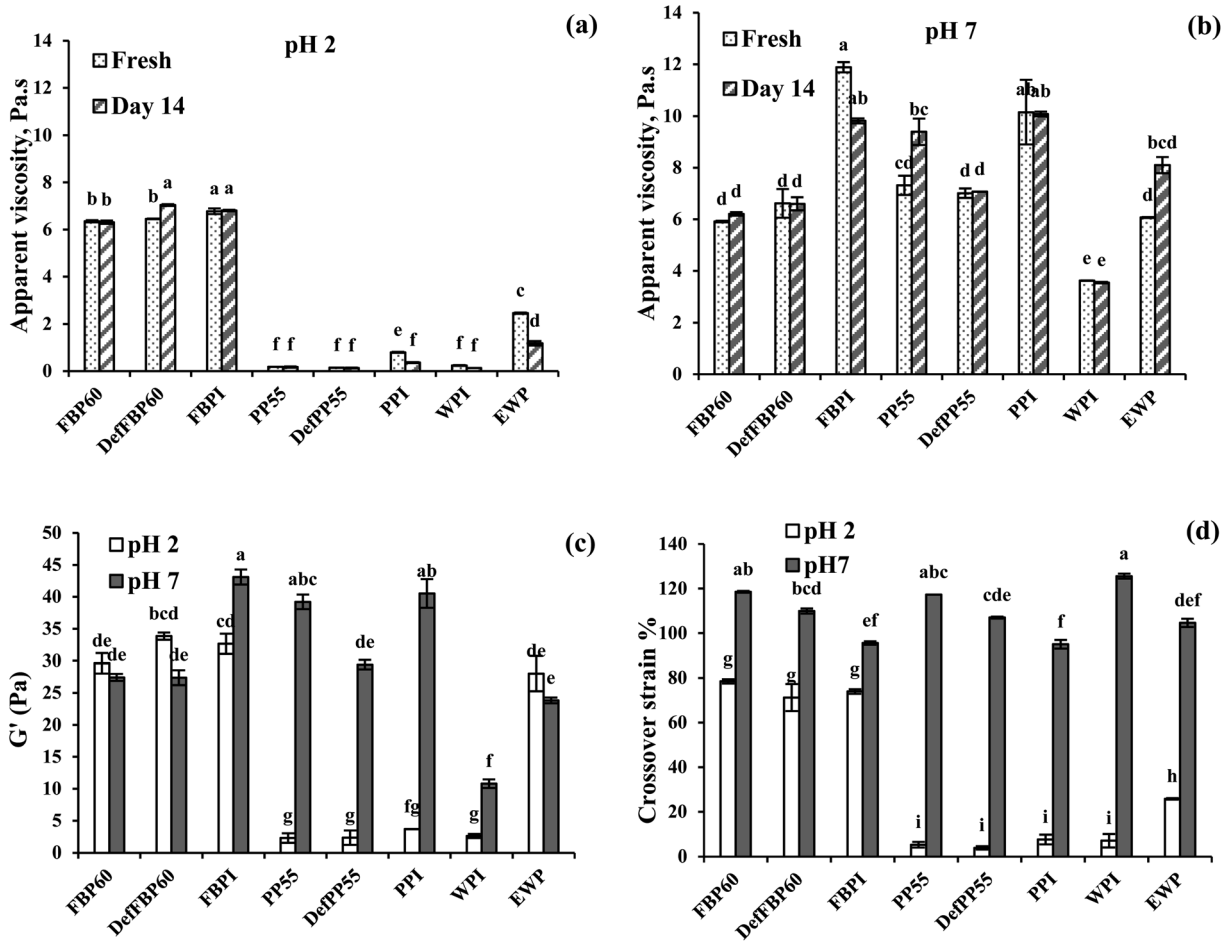

Fig. 9 Effect of storage time on the apparent viscosities (at 1 s^{-1} shear rate) of emulsions stabilized by various commercial protein samples at (a) pH 2 and (b) pH 7. Viscoelasticity of emulsions stabilized by various commercial protein samples expressed as (c) plateau storage modulus (G') at 0.1% strain and (d) crossover strain% pH2 and pH 7. Means that do not share a letter are significantly different by Tukey's test at $p < 0.05$ significance level. See Table 1 for sample identification.

their higher viscosities as emulsions with smaller droplets have more hydrodynamic interactions between the droplets.[65] At pH 7, among the different varieties, both the protein isolates showed higher viscosities than other protein types. FBPI-stabilized emulsion showed the highest apparent viscosity (11.9 ± 0.2 Pa s), followed by PPI (10.2 ± 1.2 Pa s) (Fig. 9b). This can be due to the higher protein content in the isolates than other pulse proteins. The viscosity of most emulsions stayed unchanged after 14 days at pH 2; however, the viscosity of PPI, WPI and EWP decreased (Fig. 9a). At pH 7, no change in apparent viscosity was observed for most emulsions after 14 days of storage, indicating unchanged emulsion structure with time, except the FBPI, PP55 and EWP-stabilized emulsions (Fig. 9b).

Emulsion viscoelasticity. All emulsions at pH 7 and only the FBP emulsions at pH 2 with $G' > 10$ Pa showed a linear viscoelastic region (LVR) where the storage (G') and loss modulus (G'') remained constant as a function of strain (Fig. S1, ESI†). The PP and WPI emulsions at pH 2 did not show any LVR, and the G' values were less than 5 Pa and only briefly higher than G'', indicating weak gels (Fig. S1†). At a higher strain beyond LVR, G' and G'' crossed over, indicating gel breakdown. The strain at the crossover is a measure of the force required for gel breakdown. To directly compare the gel strength of all emulsions, their G' within the LVR at 0.1% strain and the crossover strain were plotted in Fig. 9c and d, respectively. At pH 2, FBP and EWP-stabilized emulsions showed a much higher G' than PP and WPI-stabilized emulsions. Among the different FBP emulsions, no significant difference in G' was observed (Fig. 9c). At pH 2, FBP emulsions also showed much higher crossover strain than PP, WPI and EWP emulsions, indicating these emulsions can withstand higher stress before breaking down (Fig. 9d). At pH 7, the storage moduli of all PP, FBPI and WPI-stabilized emulsions was noticeably increased compared to pH 2, which shows the formation of a stronger structure (Fig. 9c). The crossover strain of all emulsions was also higher at pH 7 than pH 2. It has previously been reported that a decrease in droplet size would lead to an increase in modulus and fracture strain in emulsions.[66] In the present case, FBPI and PPI had higher protein content compared to concentrates, and de-flavoured samples and also droplet size of FBP emulsions were much smaller at pH 2 compared to PP emulsions leading to a higher gel strength. At

pH 7, all pulse protein emulsion showed strong-gel behaviour and their gel strength was higher than WPI and EWP emulsions. Gelation in pulse protein-stabilized coarse emulsions could be important for many food applications (*e.g.*, salad dressing, spreadable dipping sauce, mayonnaise, *etc.*) that requires structure formation. From the results obtained above, depending on pH and protein type, pulse proteins can be successfully used for this purpose.

3.4.5. Accelerated destabilization of emulsions. Fig. 10 shows the percent destabilization in terms of percent free oil separation under centrifugal force (2000 × *g*) for all emulsions, which can be used to predict the long-term stability of emulsion against gravitational separation and coalescence. The results of accelerated destabilization followed the trends in emulsion average particle size, where at pH 2 FBP-stabilized emulsions showed lower destabilization compared to two PP (de-flavoured and isolate), WPI and EWP-stabilized emulsions. Only PP55 showed lower destabilization at pH 2 in spite of the larger average particle size. Overall, at pH 2, DefPP55 showed the highest destabilization (34.2 ± 0.0%), followed by PPI and WPI emulsions. At pH 7, emulsion stability was significantly higher than pH 2 for most emulsions, which can be related to lower droplet size (Fig. 5 and 8) and higher magnitude of zeta potential at pH 7 (Fig. 7). Among the different FBP, at pH 2, the isolate showed slightly lower destabilization than the concentrates, but at pH 7, no difference was observed. For PP, a similar trend was observed at pH 7; however, at pH 2, only the concentrate remained stable.

3.5. Development of an empirical model to predict emulsion characteristics from protein properties

The regression models were obtained by fitting eqn (5) to the experimental data of proteins (input variables: *S*, OHC, WHC, IT, and IF (soluble + insoluble)) and emulsion (output response: droplet size, percent destabilization, and viscosity) properties (eqn (6)–(8)) at pH 7. Other input variables determined in this research (secondary structure, zeta potential) did not have any significant effect on the emulsion properties, hence was not included in the model development. The high correlation coefficient (R^2 = 0.9996, 0.9993 and 0.9994 for size, destabilization and viscosity, respectively) between the values predicted by the regression models (eqn (6)–(8)) and the experimental data implies that the EPR technique has promising potential to predict the performance of such systems (Fig. S2, ESI†).

$$\text{Size} = -0.00319 \times \text{OHC}^2 + 0.00017 \times \text{IT}^{0.5} \times \text{WHC} \times \text{IF} - 0.01281 \times S^{0.5} \times \text{WHC} \times \text{IF}^{0.5} + 40.95 \quad (6)$$

$$\text{Destabilization} = 0.58509 \times \text{IF}^2 + 0.01929 \times \text{IT}^{0.5} \times \text{IF}^{0.5} + 0.00011 \times S^2 \times \text{IT}^{0.5} - 2.2385 \quad (7)$$

$$\text{Viscosity} = 0.00731 \times \text{WHC} \times \text{IF}^{0.5} + 1.73 \times 10^{-8} \times \text{WHC}^2 \times \text{OHC}^2 \times \text{IF}^{0.5} + 0.00289 \times S \times \text{IT}^{0.5} + 3.3194 \quad (8)$$

To investigate the strength of the relationship between the input (*S*, OHC, WHC, IF, and IT) and output (emulsion droplet size, destabilization and viscosity) parameters, the traditional and widely used one-factor-at-a-time (OFAT) approach was employed. The analysis was conducted such that one variable of eqn (6)–(8) was changed step by step from a low to a high value at one time, while the other variables were kept fixed at their baseline values. Then, the selected variable was returned to its baseline value, and these steps were repeated for each of the other inputs in the same way. In order to make a tangible comparison between the input and output parameters, the range of values obtained for *S* (8.25–100%), IF (5.16×10^6 to 2.74×10^7), IT (6.65–15.40 mN m^{-1}), WHC (1.16–5.56 g g^{-1}) and OHC (0.73–1.15 g g^{-1}) were normalized between 1 and 100. The mean normalized value of *S* (50.89), IF (61.44), IT (49.79), WHC (42.84) and OHC (40.34) were considered as the baselines in the OFAT analysis. Fig. 11a, b and c show the variations in the emulsion droplet size, destabilization and viscosity,

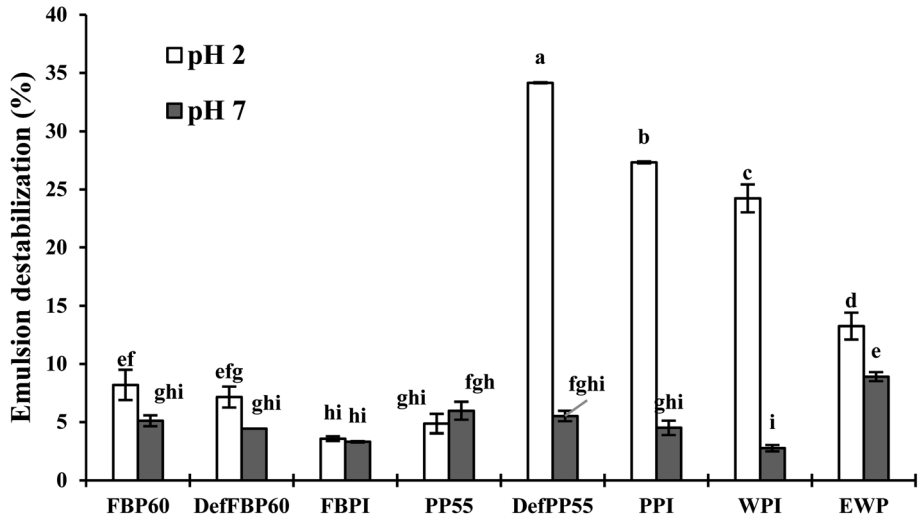

Fig. 10 Percent emulsion destabilization in terms of free oil separation under centrifugal force. Emulsions were prepared with various commercial protein samples at pH 2 and pH 7. Means that do not share a letter are significantly different by Tukey's test at $p < 0.05$ significance level. See Table 1 for sample identification.

respectively, as a function of the input variables based on eqn (6)–(8). It should be noted that only a specific range of values for each input parameter is shown where the model predictions are reasonable. As shown in Fig. 11a, WHC had the highest effect (slope of −0.64) on the emulsion particle size, such that when WHC increased from its minimum to maximum value, the emulsion particle size decreased from 28.7 to 9.6 μm. Increasing OHC, IF, and *S* also led to the reduction in emulsion particle size (slopes −0.1, −0.37, and −0.51, respectively). As expected, IT had the opposite effect, although an increase from the minimum to maximum value showed a minor increase in emulsion particle size from 8.2 to 9.5 μm (slope of 0.02). For emulsion destabilization (Fig. 11b), solubility had the highest effect (slope of 0.06) on the emulsion size, followed by IF (slope of 0.05) and IT (slope of 0.03). As these parameters were increased from minimum to maximum value, the emulsion destabilization increased. Emulsion viscosity was mostly affected by WHC (slope of 0.08), whose effect was higher than IF, OHC, *S* and IT (slope of 0.03, 0.02, 0.02 and 0.01, respectively) (Fig. 11c) increasing all these factors from minimum to maximum increased emulsion viscosity.

Overall, our model predicts that an increase in protein *S*, WHC, OHC and IF are more favourable to decrease emulsion particle size. However, it also predicts that an increase in *S* and IF in the given range would lead to higher emulsion destabilization under accelerated gravity. It is possible that if proteins are more soluble in the aqueous phase, they could be removed from the oil droplet surface during centrifugal separation into the aqueous phase, leading to droplet coalescence and emulsion destabilization. From Fig. 4a, we have seen that the soluble fraction of proteins had significantly higher IF; therefore, it is reasonable that the effect of *S* is similar to IF. IT did not show much influence on emulsion particle size, although a lower value of IT seems more favourable to lower emulsion destabilization under accelerated gravitation. Lower IT indicates that proteins are more surface-active; therefore, they tend to reside at the oil droplet surface and protect the droplets from forced destabilization. For emulsion viscosity, the model predicts a positive correlation with all the input variables, although WHC of proteins seems to be the one most influencing emulsion viscosity. This means protein's ability to bind with water seems to be more critical in controlling emulsion viscosity than

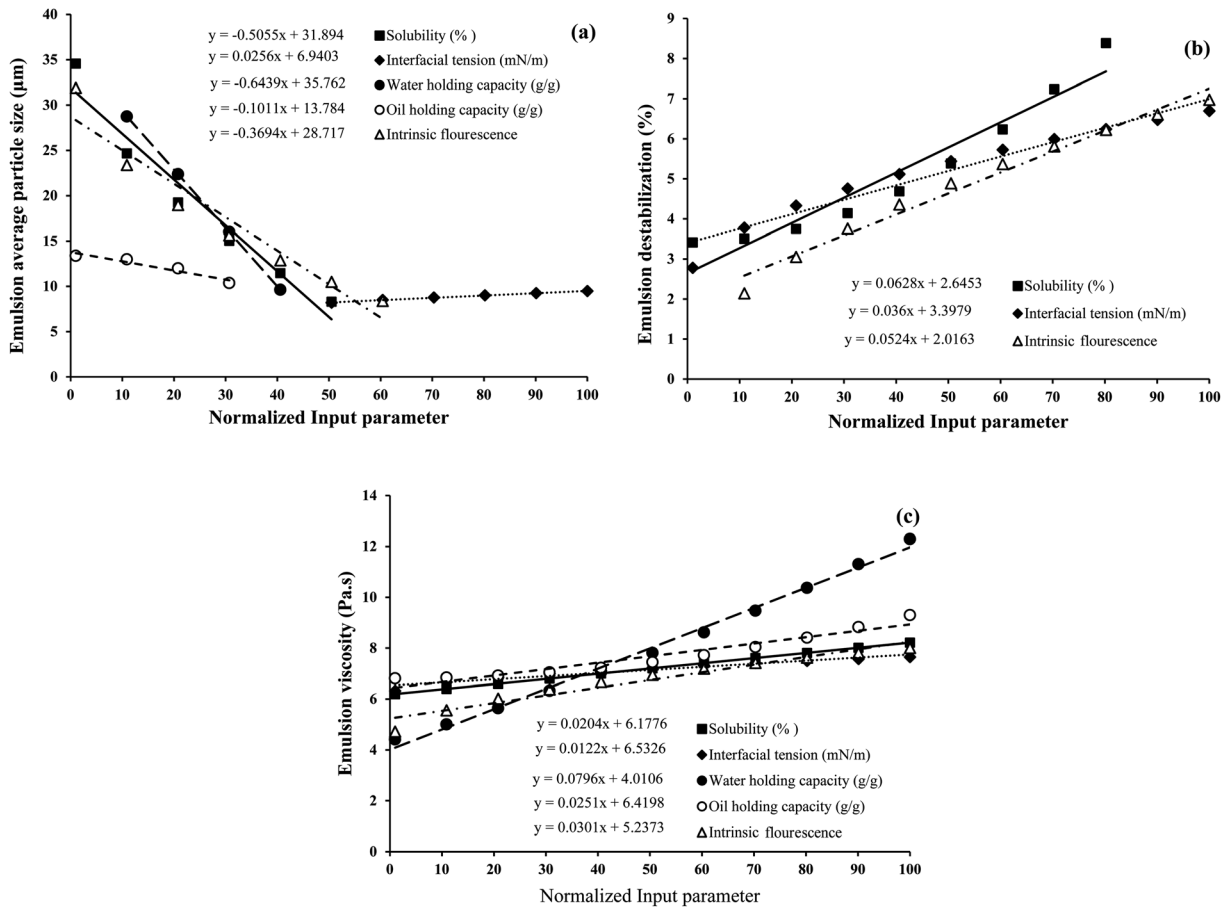

Fig. 11 Model prediction of emulsion (a) average particle size, (b) destabilization % and (c) viscosity as a function of normalized input parameters: solubility (*S*), interfacial tension (IT), water (WHC) and oil holding capacity (OHC), and intrinsic fluorescence (IF). The strength of the relationship between the input and output (emulsion droplet size, destabilization and viscosity) parameters was investigated using the one-factor-at-a-time (OFAT) approach, where one input variable was changed step-by-step from a low to a high value at one time, while the other variables were kept fixed at their mean normalized baseline values.

their other properties. Finally, it should be mentioned that the empirical model proposed here is based on the input variables determined at pH 7, and the model is only valid for the used ranges for all the variables. However, such an approach would certainly be useful to predict emulsion formation and the stabilization of various protein ingredients for the food industry.

4. Conclusions

An extensive study was done to compare the structure, functionality and emulsification behaviour of isolates, concentrates and de-flavoured concentrates of PP and FBP in comparison with WPI and EWP at neutral (pH 7) and acidic (pH 2) conditions. Protein concentrates showed significantly higher solubility compared to the isolates. The solubility of WPI and EWP, however, was significantly higher than all the pulse protein samples. The SDS-PAGE profiles of the protein concentrates showed the presence of more high-molecular-weight bands in the soluble compared to the insoluble fractions; however, for the isolates, not much difference was observed. The protein secondary structure did not show a consistent difference between the various samples. In contrast, IF of the soluble fractions showed much higher intensity compared to the insoluble fractions, indicating the protein's ability to hide the aromatic amino acids in the hydrophobic interior, thereby lower quenching of their fluorescence in the aqueous phase. IT of all plant proteins were comparable to WPI and EWP. All samples of FBP showed a lowering of IT at pH 7 compared to pH 2, while no significant difference was observed for PP, which remained higher than FBP. The higher protein content of the isolates was found to improve their WHC. The zeta potential of all proteins was higher at pH 7 than pH 2, and the isolates had higher charges compared to the concentrates. At pH 7, all plant proteins showed higher zeta potential than WPI and EWP.

All emulsions prepared at pH 7, were more stable than the ones at pH 2, which led to higher viscosities and storage moduli at pH 7 compared to pH 2. The contrasting effect of pH on emulsion stability and viscosity was more noticeable for PP compared to the FBP; therefore, the latter is more suitable for both pH values, even when compared with WPI and EWP. Emulsions stabilized with the concentrates appeared to be better or comparable to the isolates in terms of particle size, zeta potential, and microstructure. The isolate-stabilized emulsions, however, had higher viscosity compared to the concentrates at pH 7, while at pH 2, no such difference was observed. Heat treatment led to a particle size increase in all emulsions. The addition of salt had a greater destabilizing effect at pH 2 compared to pH 7. Once again, FBP appeared as more suitable for emulsion stability when both heat treatment and salt addition was compared.

Finally, the EPR technique was successfully used to develop empirical models to predict emulsion particle size, destabilization and viscosity at pH 7 based on S, OHC, WHC, IF, and IT. It was found that an increase in protein S, WHC, OHC and IF are more favourable to decrease emulsion particle size, while an increase in S and IF in the given range would lead to higher emulsion destabilization under accelerated gravity. A decrease in IT, while did not have much influence on emulsion particle size, was more favourable to lower emulsion destabilization under accelerated gravitation. Emulsion viscosity was more dependent on WHC compared to any other factors. Such an approach, although with limited ability, could be useful for ingredient manufacturers to predict the emulsification ability of their protein ingredients based on their physicochemical properties.

Conflicts of interest

There are no conflicts to declare.

Acknowledgements

This research was supported by NSERC Engage Grant in collaboration with AGT Foods, Canada, and Canada Foundation for Innovation (CFI) Leaders Opportunity Fund and Saskatchewan Science foundation.

References

1 A. C. Y. Lam, A. Can Karaca, R. T. Tyler and M. T. Nickerson, *Food Rev. Int.*, 2018, **34**, 126–147.
2 M. Duranti and C. Gius, *Field Crops Res.*, 1997, **53**, 31–45.
3 Y. Ladjal-Ettoumi, H. Boudries, M. Chibane and A. Romero, *Food Biophys.*, 2016, **11**, 43–51.
4 M. Carbonaro, P. Maselli and A. Nucara, *Amino Acids*, 2012, **43**, 911–921.
5 M. Carbonaro, P. Maselli and A. Nucara, *Food Res. Int.*, 2015, **76**, 19–30.
6 A. C. Karaca, N. Low and M. Nickerson, *Food Res. Int.*, 2011, **44**, 2742–2750.
7 P. Pelgrom, J. Wang, R. Boom and M. Schutyser, *J. Food Eng.*, 2015, **155**, 53–61.
8 A. K. Stone, A. Karalash, R. T. Tyler, T. D. Warkentin and M. T. Nickerson, *Food Res. Int.*, 2015, **76**, 31–38.
9 J. Boye, F. Zare and A. Pletch, *Food Res. Int.*, 2010, **43**, 414–431.
10 P. Pelgrom, A. Vissers, R. Boom, M. Schutyser, P. Pelgrom, A. Vissers, R. Boom and M. Schutyser, *Food Res. Int.*, 2013, **53**, 232–239.
11 R. Aluko and R. Yada, *Int. J. Food Sci. Nutr.*, 1997, **48**, 31–39.
12 X. Han and B. R. Hamaker, *Starch*, 2002, **54**, 454–460.
13 Z. Ma, J. Boye, B. Simpson, S. Prasher, D. Monpetit and L. Malcolmson, *Food Res. Int.*, 2011, **44**, 2534–2544.
14 A. Singhal, A. C. Karaca, R. Tyler and M. Nickerson, in *Grain Legumes*, InTech, 2016.
15 J. E. Kinsella and N. Melachouris, *Crit. Rev. Food Sci. Nutr.*, 1976, **7**(3), 219–280.
16 B. Nagmani and J. Prakash, *Int. J. Food Sci. Nutr.*, 1997, **48**, 205–214.
17 M. Vogelsang-o, I. L. Petersen, M. S. Joehnke, J. C. Sørensen, J. Bez, A. Detzel, M. Busch, M. Krueger, J. A. O. Mahony, E. K. Arendt and E. Zannini, *Foods*, 2020, **9**, 1–24.
18 N. Diftis and V. Kiosseoglou, *Food Chem.*, 2003, **81**, 1–6.

19 R. Aluko, O. Mofolasayo and B. Watts, *J. Agric. Food Chem.*, 2009, **57**, 9793–9800.
20 M. P. Aronson, *Langmuir*, 1989, **5**, 494–501.
21 S. D. Arntfield and E. D. Murray, *Can. Inst. Food Sci. Technol. J.*, 1981, **14**, 289–294.
22 Z. Q. Jiang, M. Pulkkinen, Y. J. Wang, A. M. Lampi, F. L. Stoddard, H. Salovaara, V. Piironen and T. Sontag-Strohm, *LWT–Food Sci. Technol.*, 2016, **68**, 295–305.
23 A. V. Megha and D. R. Grant, *Can. Inst. Food Sci. Technol. J.*, 1986, **19**, 174–180.
24 V. B. Galazka, E. Dickinson and D. A. Ledward, *Food Hydrocolloids*, 1999, **13**, 425–435.
25 W. Peng, X. Kong, Y. Chen, C. Zhang, Y. Yang and Y. Hua, *Food Hydrocolloids*, 2016, **52**, 301–310.
26 S. T. Ohnishi and J. K. Barr, *Anal. Biochem.*, 1978, **86**, 193–200.
27 C. D. Doan and S. Ghosh, *Nanomaterials*, 2019, **9**, 2–4.
28 M. Yerramilli, N. Longmore and S. Ghosh, *Food Hydrocolloids*, 2017, **64**, 99–111.
29 M. Carbonaro and A. Nucara, *Amino Acids*, 2010, **38**, 679–690.
30 Q. Yan, *Bio-protocol*, 2011, **1**, 1–2.
31 S. Pahlavanzadeh, K. Zoroufchi Benis, M. Shakerkhatibi, A. Karimi Jashni, N. Taleb Beydokhti and S. Alizadeh Kordkandi, *J. Environ. Chem. Eng.*, 2018, **6**, 6154–6164.
32 O. Giustolisi and D. A. Savic, *J. Hydroinf.*, 2006, **8**, 207–222.
33 M. Najafzadeh and M. Zeinolabedini, *Environ. Sci. Pollut. Res.*, 2018, **25**, 22931–22943.
34 S. Alzabeebee and D. N. Chapman, *Transp. Geotech.*, 2020, **24**, 100372.
35 M. Shakerkhatibi, N. Mohammadi, K. Zoroufchi Benis, A. B. Sarand, E. Fatehifar and A. A. Hashemi, *Environ. Health Eng. Manage. J.*, 2015, **2**, 117–122.
36 Kh. Zoroufchi Benis, M. Shakouri, K. McPhedran and J. Soltan, *Environ. Sci. Pollut. Res.*, 2021, **28**, 12659–12676.
37 D. Laucelli and O. Giustolisi, *Environ. Model. Softw.*, 2011, **26**, 498–509.
38 X. Qu and C. F. J. Wu, *J. Stat. Plan. Inference*, 2005, **131**, 407–416.
39 F. Sosulski and A. McCurdy, *J. Food Sci.*, 1987, **52**, 1010–1014.
40 N. Leyva-Lopez, N. Vasco, A. Barba de la Rosa and O. Paredes-Lopez, *Plant Foods Hum. Nutr.*, 1995, **47**, 49–53.
41 P. J. Shand, H. Ya, Z. Pietrasik and P. K. J. P. D. Wanasundara, *Food Chem.*, 2007, **102**, 1119–1130.
42 N. J. Neucere, *J. Agric. Food Chem.*, 1972, **20**, 252–255.
43 D. J. McClements, F. J. Monahan and J. E. Kinsella, *J. Food Sci.*, 1993, **58**, 1036–1039.
44 R. A. Judge, E. L. Forsythe and M. L. Pusey, *Biotechnol. Bioeng.*, 1998, **59**, 776–785.
45 E. Derbyshire, D. J. Wright and D. Boulter, *Phytochemistry*, 1976, **15**, 3–24.
46 I. Correia, A. Nunes, A. S. Barros and I. Delgadillo, *J. Cereal Sci.*, 2010, **51**, 146–151.
47 E. Gujska and K. Khan, *J. Food Sci.*, 1991, **56**, 1013–1016.
48 H. Y. Law, S. M. Choi and C. Y. Ma, *Food Res. Int.*, 2008, **41**, 720–729.
49 C. H. Tang and C. Y. Ma, *Food Chem.*, 2009, **115**, 859–866.
50 C. H. Tang and X. Sun, *Food Hydrocolloids*, 2011, **25**, 315–324.
51 C. Chang, S. Tu, S. Ghosh and M. T. Nickerson, *Food Res. Int.*, 2015, **77**, 360–367.
52 A. Gharsallaoui, E. Cases, O. Chambin and R. Saurel, *Food Biophys.*, 2009, **4**, 273–280.
53 S. P. Johnston, M. T. Nickerson and N. H. Low, *J. Food Sci. Technol.*, 2015, **52**, 4135–4145.
54 R. Toews and N. Wang, *Food Res. Int.*, 2013, **52**, 445–451.
55 O. Paredes-Lopez, C. Ordorica-Falomir, M. R. Olivares-Vazquez, O. Paredes-Lopez, C. Ordorica-Falomir and M. R. Olivares-Vazquez, *J. Food Sci.*, 1991, **56**, 726–729.
56 J. Boye, S. Aksay, S. Roufik, S. Ribéreau, M. Mondor, E. Farnworth and S. Rajamohamed, *Food Res. Int.*, 2010, **43**, 537–546.
57 K. Demetriades, J. N. Coupland and D. J. McClements, *J. Food Sci.*, 1997, **62**, 342–347.
58 P.-O. Hegg, *Biochim. Biophys. Acta, Protein Struct.*, 1979, **579**, 73–87.
59 K. Shevkani, N. Singh, A. Kaur and J. C. Rana, *Food Hydrocolloids*, 2015, **43**, 679–689.
60 C. E. Gumus, E. A. Decker and D. J. Mcclements, *Food Biophys.*, 2017, **12**, 186–197.
61 E. Dickinson, *Colloids Surf., B*, 2010, **81**, 130–140.
62 H. N. Xu, Y. Liu and L. Zhang, *Soft Matter*, 2015, **11**, 5926–5932.
63 O. F. Castellani, E. N. Martínez and M. C. Añón, *J. Agric. Food Chem.*, 1998, **46**, 4846–4853.
64 M. Primozic, A. Duchek, M. Nickerson and S. Ghosh, *Food Hydrocolloids*, 2018, **77**, 126–141.
65 R. Pal, *J. Colloid Interface Sci.*, 2000, **225**, 359–366.
66 G. Sala, T. van Vliet, M. Cohen Stuart, F. van de Velde and G. A. van Aken, *Food Hydrocolloids*, 2009, **23**, 1853–1863.